

RAMoEA-QA: Hierarchical Specialization for Robust Respiratory Audio Question Answering

Gaia A. Bertolino

University of Cambridge, United Kingdom

GAB62@CAM.AC.UK

Yuwei Zhang

University of Cambridge, United Kingdom

YZ798@CAM.AC.UK

Tong Xia

Tsinghua University, China

TONGXIA@MAIL.TSINGHUA.EDU.CN

Domenico Talia

University of Calabria, Italy

TALIA@DIMES.UNICAL.IT

Cecilia Mascolo

University of Cambridge, United Kingdom

CM542@CAM.AC.UK

Abstract

Conversational generative AI is rapidly entering healthcare, where general-purpose models must integrate heterogeneous patient signals and support diverse interaction styles while producing clinically meaningful outputs. In respiratory care, non-invasive audio, such as recordings captured via mobile microphones, enables scalable screening and longitudinal monitoring, but the heterogeneity challenge is particularly acute: recordings vary widely across devices, environments, and acquisition protocols, and questions span multiple intents and question formats. Existing biomedical audio-language QA systems are typically monolithic, without any specialization mechanisms for tackling diverse respiratory corpora and query intents. They are also only validated in limited settings, leaving it unclear how reliably they handle the shifts encountered in real-world settings. To address these limitations, we introduce **RAMoEA-QA**, a hierarchically routed generative model for *respiratory audio question answering* that unifies multiple question types and supports both discrete and continuous targets within a single multimodal system. RAMoEA-QA applies two-stage conditional specialization: an **Audio Mixture-of-Experts** routes each recording to a suitable pre-trained audio encoder, and a **Language Mixture-of-Adapters** selects a LoRA adapter on

a shared frozen LLM to match the query intent and answer format. By specializing both acoustic representations and generation behaviour per example, RAMoEA-QA consistently outperforms strong baselines and routing ablations with minimal parameter overhead, improving in-domain test accuracy to 0.72 (vs. 0.61 and 0.67 for state-of-the-art baselines) and exhibiting the strongest generalization for diagnosis under domain, modality, and task shifts.

Data and Code Availability We use respiratory audio question-answer pairs from the RA-QA collection (Bertolino et al., 2026), which aggregates multiple open-source respiratory audio datasets and their associated metadata. Data access follows the original dataset licenses. Our code is available at this [link](#).

Institutional Review Board (IRB) This study obtained IRB approval from the relevant boards to work with the public and controlled access data described.

1. Introduction

Respiratory diseases remain a leading cause of global morbidity and mortality, motivating early, accessible, and scalable screening tools, especially for telemedicine and low-resource settings (Labaki and Han, 2020). In clinical practice, respiratory sound assessment provides diagnos-

tic cues (e.g., wheezes, crackles, timing patterns) for conditions such as asthma, pneumonia, and chronic obstructive pulmonary disease (COPD). Recent machine learning work has achieved strong results for respiratory sound classification from recordings and has enabled reusable pretrained audio backbones for downstream respiratory tasks (Reichert et al., 2008; Sovijärvi et al., 1999; Zhang et al., 2024).

Despite the progress, existing systems typically produce a single, task-specific output (e.g., disease label or abnormality detection), which limits their usefulness in real clinical interactions. In practice, respiratory assessment is inherently driven by different questions iteratively: clinicians and patients seek different, context-dependent information from the same recording (e.g., *Is wheezing present?*, *Which diagnosis is most likely?*, *How severe is it?*) Enabling flexible question answering over respiratory audio would allow *interactive* respiratory assessment beyond a single, static prediction. Although general-purpose multimodal assistants are increasingly explored for conversational healthcare support (Munikoti et al., 2024; OpenAI, 2026; Anthropic, 2026; Google AI, n.d.), and clinical QA has been widely studied for modalities such as electronic health records, medical imaging, and biosignals (Pampari et al., 2018; Nguyen et al., 2023; Oh et al., 2023), conversational AI for respiratory audio remains under-explored.

Existing large-scale audio-language foundation models (Deshmukh et al., 2024b; Das et al., 2024; Chu et al., 2023) have proven to be strong for generic audio understanding, yet they are unreliable for respiratory assessment (Wang et al., 2025). This limitation stems from the lack of training on respiratory acoustics and clinical knowledge, where cues are subtle, recordings are uncontrolled, and sound-label relationships are noisy and context-dependent. Early biomedical audio-language QA models partially address these limitations but are developed and validated in relatively constrained settings (e.g., limited question formats and target types), and rarely study how to specialize across diverse respiratory corpora and query intents, which is crucial because real-world respiratory audio question-answering must generalize across question-types, *modality* (cough/breath/speech), *dataset/device*, and *task* shifts, thus leaving it unclear whether

a single monolithic pathway can reliably support the diversity of clinically structured questions encountered in practice (Wang et al., 2025).

To address these limitations, we introduce **RAMoEA-QA**, a hierarchically routed generative model for respiratory audio question answering that supports multiple question types and both discrete and continuous targets within a single multimodal system. RAMoEA-QA applies two-stage conditional specialization: an **Audio Mixture-of-Experts** routes each recording to a suitable pre-trained audio encoder, and a **Language Mixture-of-Adapters** selects a LoRA adapter on a shared frozen LLM to match the query intent and answer format.

We evaluate our approach on the **RA-QA collection** (Bertolino et al., 2026), a multi-dataset benchmark spanning three question formats (*open-ended*, *single-verify*, *multiple-choice*) and two task families (*diagnosis*, including *severity assessment*, and *regression*). Beyond in-distribution evaluation, we conduct controlled robustness tests under **modality**, **dataset**, and **task** shift, and provide routing analyses that characterize specialization patterns and diagnose/mitigate routing collapse via expert heterogeneity and routing stabilization.

Contributions. This paper makes the following contributions:

- We propose **RAMoEA-QA**, a **two-stage routed** architecture that activates one audio encoder expert (Audio-MoE) and one LoRA adapter on a shared frozen LLM (Language-MoA) per example. This enables hierarchical specialization with minimal overhead, supporting multi-dataset, multi-task, and multi-format respiratory-audio question-answering.
- We systematically study respiratory audio QA by benchmarking against a generic audio QA model and single-path biomedical QA baselines on the RA-QA collection, covering open-ended, single-verify, and multiple-choice questions across diagnosis, severity, and regression targets.
- Our experiments show consistent gains over strong baselines on both discriminative and regression tasks, improving discriminative

accuracy by 12.5% on average, while exhibiting stronger generalization for diagnosis under domain, modality, and task shifts. Our routing analysis reveals that the learned router selectively leverages the benefits of different paths within a single unified model.

2. Related Work

Audio ML for respiratory health. Machine learning for respiratory acoustics has primarily focused on supervised classification and detection using cough and breath recordings, targeting tasks such as disease screening, symptom identification, and severity estimation (Gairola et al., 2021; Fraiwan et al., 2021a; Srivastava et al., 2021; Reichert et al., 2008; Sovijärvi et al., 1999). More recently, respiratory *audio foundation models* have been introduced to leverage large-scale pretraining for improved transfer across datasets and recording conditions (Zhang et al., 2024). While these approaches provide strong acoustic representations and competitive performance on standard prediction tasks, they are typically designed for fixed outputs (labels or scores) and do not directly support question-conditioned clinical interactions where the same recording may be queried in multiple ways (e.g., diagnosis, symptom verification, or severity/regression targets).

QA systems in healthcare. Clinical question answering has been extensively studied in text-centric settings, including QA over clinical notes and biomedical literature (Pampari et al., 2018; Jin et al., 2019; Nguyen et al., 2023; Tsatsaronis et al., 2015), as well as structured EHR query answering (Wang et al., 2020; Lee et al., 2023). Beyond text, multimodal medical QA benchmarks have emerged for modalities such as medical imaging and biosignals (Abacha et al.; Hu et al., 2024; Oh et al., 2023), alongside approaches that integrate large language models with modality-specific encoders for instruction following and multimodal reasoning (Singhal et al., 2022; Wu et al., 2024a). More broadly, recent work emphasizes a shift toward *generalist* assistants that aim to handle diverse modalities, tasks, and interaction styles within a single interface, including emerging healthcare-facing conversational systems (Munikoti et al., 2024; OpenAI, 2026; Anthropic, 2026; Google AI, n.d.).

In the audio domain, general-purpose audio-language models have demonstrated broad capabilities across tasks (Deshmukh et al., 2024b; Das et al., 2024; Chu et al., 2023; Gong et al., 2024; Ghosh et al., 2024; Huang et al., 2023). More recently, respiratory-focused resources such as CareAQA (Wang et al., 2025) have targeted biomedical audio question answering, but they typically emphasize a narrower set of respiratory objectives rather than robust, multi-format clinical querying. This leaves a gap between generalist conversational systems and clinically grounded respiratory audio QA: practical assistants must handle heterogeneous question styles (open-ended explanations, verification, multiple-choice) and task families (discriminative and regression-style severity targets) under dataset and recording-condition shift. Prior respiratory audio QA systems remain limited in scale and scope, and they rarely study conditional specialization across heterogeneous respiratory data and query types, nor integrated uncertainty signals that could support safer clinical behaviour.

MoE/MoA architectures for specialization, efficiency, and robustness. Mixture-of-Experts (MoE) enable conditional computation by routing each input to a subset of experts, improving scalability and capacity while controlling computation (Jacobs et al., 1991; Lepikhin et al., 2020; Fedus et al., 2022). In parallel, parameter-efficient fine-tuning methods such as adapters and LoRA have made it practical to adapt large pretrained models without updating all parameters (Pfeiffer et al., 2021; Hu et al., 2021). Building on these ideas, mixture-of-adapters (often referred to as MoA) train multiple lightweight adapters that are dynamically selected at inference time, enabling modular specialization with limited trainable parameters (Lee et al., 2024; Buehler and Buehler, 2024; Wu et al., 2024b; Wang and Li, 2024). Beyond efficiency, conditional specialization can improve *robustness under distribution shifts* by activating experts aligned to the current input domain (e.g., device, modality, cohort) or query formats, rather than forcing a single parameterization to fit all conditions (Guo et al., 2018). A known challenge in mixture-based systems is *routing imbalance* and collapse, where a small subset of experts receives most of the traffic and parame-

ters are effectively under-utilized; prior work has studied load-balancing, entropy regularization, and related stabilization strategies in sparse mixtures (Fedus et al., 2022; Lepikhin et al., 2020). Despite their success in NLP, MoE and MoA have been less explored as *joint* mechanisms for specialization in multimodal clinical QA, particularly for respiratory audio, where both acoustic variability and heterogeneous question formats motivate hierarchical specialization.

3. Method

This section presents *RAMoEA-QA* as a two-stage conditional-specialization model for respiratory audio question answering (RA-QA). Given an audio recording and a natural-language question, the model generates a short answer whose *format and target* are defined by the question (e.g., diagnosis/severity as discrete labels or spirometry/physiology as a numeric value).

3.1. Overview

Our key principle is *hierarchical specialization* under constrained resources: we activate *one* acoustic pathway and *one* generation pathway per example (hard top-1 routing), achieving conditional computation without mixing experts. Figure 1 summarizes the full flow and highlights the two routing stages: **(A) Audio-MoE** and **(B) LoRA-MoA**. Concretely, (A) we compute a lightweight routing representation from the input and select a single pre-trained audio encoder expert; its output is aligned to the LLM hidden size and injected as a *selected audio prefix* (aligned audio embeddings concatenated into the LLM input). (B) conditioned on the question and the selected aligned audio prefix, we select a single LoRA adapter attached to a shared frozen LLM backbone and generate the answer.

3.2. Routing configuration and policies

In our setting, *routing* denotes the expert *selection mechanism*: which audio encoder (Audio-MoE) and which language adapter (MoA) are activated for a given input pair. The routing *configuration* refers to the *router-input policy* used to compute gating logits: **audio**, **question**, or

fused. This choice does *not* change what the experts themselves receive (audio encoders always process the spectrogram; the LLM always processes the prompt plus the selected aligned audio prefix). Instead, it only specifies which representation is fed to each router: an audio-only summary, a question-only summary, or a fused question-audio summary.

Routing is trained with straight-through Gumbel-Softmax for expert exploration and evaluated in inference with argmax selection; we use a short balanced warmup to prevent routing collapse and keep router temperatures and auxiliary weights fixed across experiments unless explicitly ablated.

3.3. Audio Mixture-of-Experts (Audio-MoE)

Lightweight routing proxy. As illustrated in the **orange** block in Fig. 1, the router directs the audio recording towards one of the available experts. To avoid running all audio encoders, the Audio-MoE first computes a low-cost *routing proxy* from the spectrogram and (optionally) the question, and uses it to select a single audio expert. We support three router-input policies (**audio/question/fused**); **fused** enables question-conditioned expert selection using the proxy rather than any full expert output.

Expert activation and alignment. Let $\{\mathcal{E}_1^a, \dots, \mathcal{E}_{N_a}^a\}$ be heterogeneous pre-trained audio encoders used as *frozen* foundation backbones. After the router selects an expert, only the chosen encoder processes the spectrogram, producing an embedding sequence that is mapped to the LLM hidden size via an expert-specific aligner and injected into the LLM input as a *selected audio prefix* (aligned audio embeddings concatenated into the LLM context). We do not update the audio encoders’ base parameters; instead, the audio encoding layer is *wrapped* with a lightweight LoRA-style adaptation layer so it can be specialized to RA-QA without full audio fine-tuning. Together with hard top-1 routing over a single LoRA adapter on the language side, this yields example-specific specialization while keeping inference compute close to a single-path model.

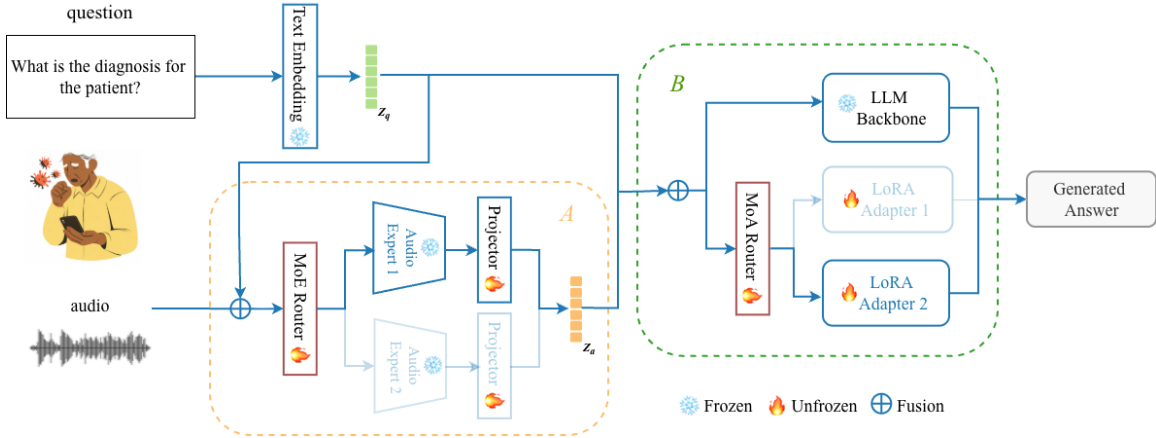


Figure 1: Two-stage routing for RA-QA. (A) The MoE selects an audio expert (encoder). The resulting aligned audio embeddings are injected as a selected audio prefix. (B) The MoA selects a LoRA adapter for the language model during generation.

3.4. Language Mixture-of-Adapters (LoRA-MoA)

Shared LLM with adapter experts. As illustrated in the green block in Fig. 1, we use a shared frozen autoregressive language backbone and attach N_ℓ LoRA adapters as lightweight language experts. The MoA router selects exactly one adapter per example, enabling specialization across question formats and task families while keeping the backbone fixed.

Router input without re-embedding. After audio expert selection and alignment, the MoA router computes its routing vector using the *same* three router-input policies (audio/question/fused), instantiated at the language stage. Here, *audio* summarizes the *selected aligned* audio prefix, *question* summarizes the prompt/question tokens, and *fused* performs a lightweight fusion between them.

Complementary two-stage fusion. Importantly, even if both routers use a *fused* configuration, they do *not* condition on the same signal: (A) fuses the question with a *cheap pre-encoder proxy* before selecting an audio expert, whereas (B) fuses the prompt with *expert-produced aligned audio embeddings* after expert selection. This staged conditioning makes routing decisions complementary (coarse acoustic/-

domain choice vs. generation/style/intent refinement), rather than redundant.

3.5. Training objective and routing regularization.

We train with teacher forcing and compute the negative log-likelihood only over answer tokens (prompt and audio-prefix positions are masked). Let $\mathcal{L}_{\text{main}}$ denote this masked language-model loss. For routing, let $\mathbf{p}_a \in \mathbb{R}^{N_a}$ and $\mathbf{p}_\ell \in \mathbb{R}^{N_\ell}$ be the softmax routing probabilities over the N_a audio experts and N_ℓ LoRA adapters, and let $\mathbf{u}_a, \mathbf{u}_\ell$ be the corresponding hard one-hot assignments (from straight-through Gumbel-Softmax during training). We add load-balancing regularization $\mathcal{L}_{\text{LB}}(\cdot)$ to encourage non-degenerate expert utilization, and optionally an entropy term $\mathcal{L}_{\text{ENT}}(\cdot)$ to control confidence/sharpness. The full objective is:

$$\begin{aligned} \mathcal{L} = & \mathcal{L}_{\text{main}} + \lambda_a \mathcal{L}_{\text{LB}}(\mathbf{p}_a, \mathbf{u}_a) + \lambda_\ell \mathcal{L}_{\text{LB}}(\mathbf{p}_\ell, \mathbf{u}_\ell) \\ & - \beta_a \mathcal{L}_{\text{ENT}}(\mathbf{p}_a) - \beta_\ell \mathcal{L}_{\text{ENT}}(\mathbf{p}_\ell), \end{aligned} \quad (1)$$

where $\lambda_a, \lambda_\ell \geq 0$ weight the load-balancing terms for the audio and language routers, and $\beta_a, \beta_\ell \geq 0$ weight the entropy regularizers. More implementation details are reported in Appendix C.

4. Experimental Setup

4.1. Datasets and tasks.

We conduct all experiments on the **RA-QA collection**, which harmonizes multiple publicly available respiratory audio datasets into a unified question-answering (QA) setting. Our training mixture comprises 7 datasets belonging to the collection, spanning different acquisition settings, modalities, and labeling schemes (Table 7). To explicitly evaluate *generalization*, we further define controlled held-out settings along three axes (Table 4): (i) **modality shift** (ΔM), where we evaluate on audio modalities not used during training for a dataset (e.g., Coswara asthma trained on cough and tested on breathing/counting/vowel); (ii) **dataset shift** (ΔD), where an entire dataset is held out from training and used only at evaluation (e.g., UK COVID-19); and (iii) **task shift** (ΔT), where we evaluate on tasks not seen in training (e.g., pneumonia).

Task families. We organize questions into two task families: **Diagnosis** (predicting a categorical respiratory condition), including presence of disease and *Severity* (predicting an ordinal/discrete severity level), and **Regression** (predicting continuous physiological values such as spirometry measures, FEV1, FVC, FEV1/FVC, and respiratory rate).

Question formats We formulate respiratory assessment as **question-conditioned prediction** from audio. Each sample consists of a recording x and a natural-language question q , and the model produces an answer \hat{y} appropriate to the query. We evaluate three question formats:

- **Open-ended (OE).** The model generates a free-form textual answer. This format is used for descriptive responses (e.g., likely condition, short clinically grounded summary) and for natural-language reporting of numeric targets.
- **Single-verify (SV).** The model answers a yes/no verification question (e.g., 'Does the patient suffer from asthma?'). We treat this as binary decision making with standardized outputs (Yes/No) for evaluation.
- **Multiple-choice (MC)** Unlike open-ended QA, multiple-choice questions explicitly enumerate the candidate labels/options in the

prompt. This is a form of prompt engineering that constrains generation to a closed set and makes the task a *selection* problem rather than free-form answering.

For discriminative tasks, when a dataset provides multiple *question formats* for the same recording (e.g., open-ended, single-verify, and/or multiple-choice), we treat each (*audio, question*) pair as a separate example and include all available formats. For regression tasks, we only present question in the open-ended format since it is the most suitable.

4.2. Baselines.

We compare our model against CareAQA-style (Wang et al., 2025) *single-path* baselines (one LoRA adapter on a frozen LLM). In addition, we include one generic audio-language QA baseline, Pengi (Deshmukh et al., 2024a), that contextualize respiratory-audio question-answering within broader audio-text modelling. We provide implementation details of the baselines in Appendix D.

4.3. Evaluation Metrics

We follow the RA-QA protocol (Bertolino et al., 2026) and report both *text-level* and *task-level* metrics to separately capture (i) how well the model matches the reference form and semantics, and (ii) whether it predicts the correct clinical label or value.

Semantic-level metrics. To evaluate answer quality at the word and semantic level, we compute **Exact Match** (strict normalized match), **TokenF1** (token overlap), **BERTScore** (semantic similarity), and **METEOR** (lexical alignment) between generated and reference answers after standard normalization. These metrics reflect complementary aspects: EM/TokenF1 emphasize surface fidelity, METEOR captures word-level matching under minor morphological variation, and BERTScore provides a semantic view that is less sensitive to paraphrasing. We report overall averages and stratify by **question-type**.

Label-correctness metrics. For *classification tasks* (the diagnosis task family), we evaluate *label correctness* by extracting the target label from the model output and comparing it to

Table 1: **Overview of the datasets** used in our training, grouped by task family, with their target tasks, available audio modalities, and supported question formats.

| Task Family | Dataset | Task | Audio condition | Question-types |
|----------------|------------------------|--|--|----------------------|
| Discriminative | Coswara | Asthma | Deep and shallow breathing | SV |
| | COUGHVID | Diagnosis (Healthy, Symptomatic, Covid-19) | Coughing | SV, OE, MC |
| | ICBHI | Diagnosis (URTI, COPD) | Four clinical recording devices | SV, OE, MC |
| | KAUH Respiratory@TR | Diagnosis (Healthy, LRTI, COPD) COPD Severity | Sound types and chest positions Recording positions | SV, OE, MC OE, MC |
| Regression | MM-Lung | Spirometry (FEV1) | Deep breathing | OE |
| | MM-Lung | Spirometry (FVC) | Deep breathing | OE |
| | Nosemic | Respiratory rate | Before and after running | OE |

the ground truth. For open-ended and multiple-choice questions, we parse the generated text to recover the predicted *diagnosis label* (e.g., by normalizing case/punctuation and matching against the dataset label set), whereas for single-verify questions we parse the output into {Yes, No}. We then compute **macro-F1** and **accuracy** over the extracted labels.

For *regression tasks*, we extract the first valid numeric value from the generated answer (if present) and compare it to the ground-truth target. We report **MAE** and **RMSE** (lower is better) computed over successfully parsed examples. We further study, and additionally report parsing coverage, i.e., the fraction of test instances for which numeric extraction succeeds.

4.4. Implementation details

All models use the same audio preprocessing pipeline, following the OPERA (Zhang et al., 2024) protocol for respiratory audio. Audio is resampled, trimmed to remove leading and trailing silence, and padded/truncated to a fixed duration; log-mel spectrograms are then computed following parameters in OPERA. Dataset splits follow the provided metadata and are subject-independent when subject IDs are available, stratified by disease label.

Optimization and decoding. We optimize with AdamW (learning rate $2 \cdot 10^{-5}$, gradient clipping 1.0) for up to 100 epochs (early stopping on the validation set). Unless stated otherwise, we train with a batch size of 4 and evaluate with a batch size of 1.

Model setting (default). Our default configuration uses two OPERA audio experts (OPERA-CT and OPERA-GT) and a shared GPT-2 backbone with LoRA adapters. Audio

experts are kept frozen and their outputs are mapped to the GPT-2 hidden size with a trainable MLP aligner.

Checkpoint selection. We select checkpoints by best in-distribution validation performance using the primary metric appropriate to the task family (MacroF1 for discriminative; MAE for regression).

5. Results

We first compare RAMoEA-QA against baselines on in-distribution RA-QA performance across question formats and task families. We then study in-domain routing behaviour, including routing distributions, uncertainty-based abstention via routing entropy, and routing-collapse ablations, and analyze how the model behaves across different question types. Finally, we evaluate robustness and generalization under controlled modality, dataset, and task shifts. Unless otherwise stated, metrics are macro-averaged across datasets within each question format and averaged over multiple training runs; per-dataset and further results are deferred to the Appendix E.

5.1. Main results

Table 2 summarizes overall performance, measured by answer correctness, of our model and the baseline methods, aggregated across discriminative and regression task families. Specifically, we compare the generic audio QA model, **Pengi**, single-path baselines **CaReAQA-style** (with OPERA-CT and OPERA-GT), and **RAMoEA-QA** (our proposed model). Dataset- and question-type specific results are provided in Appendix E. Table 3 complements this compari-

Table 2: **Main results.** We compare the strongest single-path baseline to our best two-stage routing model. **NA** indicates that no valid numeric value could be parsed from the generated answer. **Bold** indicates the best result and underlining indicates the second best.

| Model | Discriminative tasks | | | | Regression tasks | | |
|-------------------------|-----------------------------------|-----------------------------------|-----------------------------------|-----------------------------------|-----------------------------------|-----------------------------------|-----------------------------------|
| | Accuracy \uparrow | Macro F1 \uparrow | Token F1 \uparrow | Exact Match \uparrow | MAE \downarrow | RMSE \downarrow | Acc@0.5 \uparrow |
| PENGI | 0.22 \pm 0.00 | 0.21 \pm 0.00 | 0.02 \pm 0.00 | 0.000 \pm 0.00 | NA | NA | NA |
| CareAQA-operaCT | 0.61 \pm 0.01 | 0.53 \pm 0.06 | 0.83 \pm 0.01 | 0.49 \pm 0.01 | 2.61 \pm 0.16 | 3.93 \pm 0.14 | 0.23 \pm 0.00 |
| CareAQA-operaGT | <u>0.67 \pm 0.15</u> | <u>0.59 \pm 0.20</u> | <u>0.86 \pm 0.06</u> | <u>0.55 \pm 0.14</u> | <u>2.61 \pm 0.09</u> | 4.26 \pm 0.14 | 0.26 \pm 0.04 |
| RAMoEA-QA (ours) | 0.72 \pm 0.02 | 0.67 \pm 0.03 | 0.88 \pm 0.00 | 0.60 \pm 0.03 | 2.29 \pm 0.31 | 3.77 \pm 0.53 | 0.32 \pm 0.04 |

Table 3: **String-level response similarity by question type (discriminative tasks).** We report BERTScore / METEOR computed on the full generated text, stratified by question format. **Bold** indicates the best result and underlining indicates the second best.

| Model | Global | | Single-Verify | | Open-ended | | Multiple-choice | |
|-------------------------|-----------------------------------|------------------------------------|-----------------------------------|------------------------------------|-----------------------------------|------------------------------------|-----------------------------------|------------------------------------|
| | BERTScore \uparrow | METEOR \uparrow |
| PENGI | -0.01 \pm 0.00 | 2.61 \pm 0.04 | 0.03 \pm 0.00 | 4.11 \pm 0.06 | -0.09 \pm 0.00 | 0.00 \pm 0.00 | -0.08 \pm 0.00 | 0.00 \pm 0.00 |
| CareAQA-operaCT | <u>0.87 \pm 0.01</u> | 84.89 \pm 0.90 | 0.87 \pm 0.02 | 86.08 \pm 1.74 | <u>0.86 \pm 0.00</u> | <u>83.15 \pm 0.87</u> | 0.85 \pm 0.02 | <u>82.96 \pm 1.83</u> |
| CareAQA-operaGT | 0.89 \pm 0.05 | <u>87.05 \pm 5.85</u> | <u>0.91 \pm 0.01</u> | <u>89.95 \pm 9.36</u> | 0.87 \pm 0.00 | 83.22 \pm 1.32 | <u>0.84 \pm 0.00</u> | 81.72 \pm 0.74 |
| RAMoEA-QA (ours) | 0.90 \pm 0.01 | 88.38 \pm 0.92 | 0.94 \pm 0.00 | 92.64 \pm 0.53 | 0.83 \pm 0.01 | 81.02 \pm 1.63 | 0.85 \pm 0.02 | 83.17 \pm 2.68 |

son with a fine-grained semantic-level analysis (BERTScore/METEOR) across question types.

Discriminative tasks. First, general audio QA models like Pengi fail to perform effectively on respiratory audio QA questions due to limited exposure to respiratory sounds and domain knowledge. As shown in Table 3, Pengi often produces irrelevant responses, resulting in extremely low word-overlap and semantic similarity scores. Moreover, within models adapted for the RA-QA collection, two-stage routing consistently improves diagnosis performance over single-path baselines. As shown in Table 2, our best configuration increases MacroF1 from 0.53 (OPERA-CT plus 1 LoRA adapter) and 0.59 (OPERA-GT plus 1 LoRA adapter) to 0.67, while also improving Accuracy (0.61 and 0.67 \rightarrow 0.72) and Exact Match (0.49 and 0.55 \rightarrow 0.60). Token-level agreement also increases (0.83 and 0.86 \rightarrow 0.88), indicating more faithful short-answer generation beyond label extraction.

Regression tasks. Generic audio QA models again fail in the regression setting: **Pengi** is unable to produce meaningful numerical predictions, and no valid numeric values can be reliably parsed from its outputs. Focusing instead on respiratory audio QA models, our two-stage

routing mechanism also consistently improves regression performance. As shown in Table 2, the strongest single-path baselines achieve an MAE of 2.61, whereas our routed model reduces error to an MAE of 2.29.

Following common practice in biomedical measurement validation (O’Brien et al., 2001; Elgendi et al., 2024), we complement MAE/RMSE with tolerance accuracy Acc@ τ , i.e., the cumulative fraction of predictions whose absolute error falls within a clinically meaningful threshold τ . Figure 2 shows that two-stage routing attains higher Acc@ τ at *stricter* tolerances on multiple spirometry and physiology targets, while converging to similar performance at looser tolerances. Together, these results indicate that conditional specialization improves both average regression quality and reliability under clinically relevant error budgets.

Response-form fidelity across question types. Table 3 evaluates format alignment across question types using BERTScore and METEOR. RAMoEA-QA achieves the highest global similarity scores, with notable gains in **single-verify** tasks (0.94 vs 92.64) due to more decisive, format-appropriate short answers. While remaining competitive on

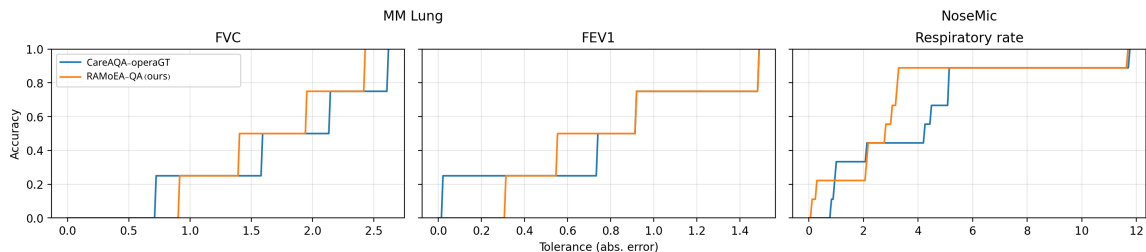


Figure 2: **Tolerance accuracy for regression.** Accuracy as a function of absolute-error tolerance ϵ for spirometry targets (FVC/FEV1 on MM-Lung) and respiratory rate (NoseMic), comparing a single-path baseline against two-stage routing. Two-stage routing reaches higher accuracy at tighter tolerances, indicating fewer large prediction errors.

multiple-choice, the model shows a slight trade-off in **open-ended** tasks, likely due to more paraphrastic generations. Overall, in addition to improving prediction correctness, routing also enhances structured response alignment demonstrated by comparative or improved semantic similarity across formats.

5.2. Robustness and generalization

We assess robustness under controlled distribution shifts by comparing the strongest single-path baseline against our RAMoEA-QA model.

Modality shift. We evaluate *unseen modality on a seen dataset and task* to probe robustness to changes of respiratory audio type within a dataset. Specifically, we test on **Coswara asthma**, trained on breathing while tested here on cough, vowels and counting, and, while all models transfer reasonably, RAMoEA-QA remains competitive and more stable across runs. On **Coswara COPD** it improves Accuracy/MacroF1 to 0.91/0.92 versus 0.68/0.75 (best baseline).

Dataset shift. We evaluate *task seen during train but on an unseen dataset* to quantify transfer under cohort/device shift while keeping the question semantics fixed. Concretely, we test on **UK COVID-19** using asthma and COVID questions. RAMoEA-QA improves both tasks under this shift, reaching 0.88/0.88 on asthma and 0.84/0.84 on COVID, outperforming the strongest single-path baselines in both

cases. This suggests that conditional specialization helps mitigate cohort/device differences when transferring to a new acquisition domain.

Task and modality shift. We evaluate *an unseen task on unseen modalities* to measure zero-shot task transfer enabled by the shared generative interface. Concretely, we test **Coswara** on unseen symptom attributes (pneumonia), and our model reaches the best performance of 0.83 accuracy while one of the single-path baselines degrades to chance-level performance.

5.3. Routing analysis

To understand *why* routing helps, we analyze empirical routing distributions for our best two-stage model. Figure 3 reports the fraction of samples routed to each audio expert (OPERA-CT vs. OPERA-GT) and each language expert (LoRA adapter 1 vs. 2), stratified by dataset, question format and task.

Dataset- and format-dependent specialization. Routing is non-uniform: the model consistently prefers different experts across datasets, question formats, tasks, and diseases. This supports the hypothesis that heterogeneous respiratory corpora (acquisition setups, noise conditions, and labelling conventions) benefit from *conditional* pathways rather than a single averaged representation.

Coupled but non-redundant two-stage routing. A notable pattern is that adapter routing largely mirrors audio routing (LoRA-

Table 4: Robustness under controlled shifts. We compare single-path baselines to RAMoEA-QA under modality, dataset, and task shifts. **Bold** indicates the best result and underlining indicates the second best. **Legend:** ΔM = unseen modality; ΔD = unseen dataset; ΔT = task never seen in training.

| Shift | Dataset | Task | CareAQA-operaCT | | CareAQA-operaGT | | RAMoEA-QA (ours) | |
|-----------------------|-------------|-----------|-----------------------------------|-----------------------------------|-----------------------------------|-----------------------------------|-----------------------------------|-----------------------------------|
| | | | Accuracy \uparrow | MacroF1 \uparrow | Accuracy \uparrow | MacroF1 \uparrow | Accuracy \uparrow | MacroF1 \uparrow |
| ΔM | Coswara | Asthma | 0.90 \pm 0.13 | 0.90 \pm 0.13 | 0.66 \pm 0.47 | 0.75 \pm 0.35 | <u>0.87 \pm 0.02</u> | <u>0.87 \pm 0.02</u> |
| | | COPD | <u>0.68 \pm 0.44</u> | <u>0.75 \pm 0.34</u> | 0.66 \pm 0.47 | 0.75 \pm 0.35 | 0.91 \pm 0.02 | 0.92 \pm 0.02 |
| ΔD | UK COVID-19 | Asthma | <u>0.84 \pm 0.21</u> | <u>0.84 \pm 0.21</u> | 0.66 \pm 0.47 | 0.74 \pm 0.35 | 0.88 \pm 0.07 | 0.88 \pm 0.06 |
| | | COVID | 0.56 \pm 0.32 | 0.65 \pm 0.20 | <u>0.66 \pm 0.47</u> | <u>0.74 \pm 0.35</u> | 0.84 \pm 0.04 | 0.84 \pm 0.04 |
| $\Delta T + \Delta M$ | Coswara | Pneumonia | <u>0.77 \pm 0.31</u> | 0.79 \pm 0.28 | 0.33 \pm 0.00 | 0.50 \pm 0.00 | 0.83 \pm 0.05 | 0.84 \pm 0.04 |
| Disc. Avg. | | | <u>0.75 \pm 0.19</u> | <u>0.75 \pm 0.19</u> | 0.67 \pm 0.20 | 0.59 \pm 0.29 | 0.78 \pm 0.04 | 0.79 \pm 0.04 |

1/LoRA-2 track OPERA-CT/OPERA-GT closely), suggesting that training discovers two coherent end-to-end pipelines (audio expert plus generation adapter) rather than mixing components arbitrarily. Importantly, this does *not* make the routers redundant: even when both use a fused policy, they condition on different signals at different stages. The Audio-MoE router uses a cheap pre-encoder proxy computed before expert selection, whereas the MoA router conditions on expert-produced aligned audio embeddings (the selected audio prefix concatenated into the LLM input). This staged conditioning lets the first router make coarse acoustic/domain decisions at low cost, while the second refines generation behaviour using richer, expert-specific representations.

Routing collapse analysis. We further study *routing collapse* in the MoE and MoA layers and its downstream impact on discriminative performance (MacroF1) and regression error (MAE). We disable routing at inference by fixing an end-to-end path (audio expert \in {OPERA-CT, OPERA-GT}, LoRA \in {L1, L2}). Table 5 reports MacroF1/MAE for forced routes (fixed audio expert \times fixed LoRA). While some collapsed paths are locally competitive for certain tasks, they have a high variance across dataset-question-type combinations and typically underperform the best routed configuration. We also note that the forced routes here have a better performance on certain tasks compared to single-path models in Table 2 on their strongest tasks (e.g. OPERA-GT for classification), which shows the strength brought by specialization.

Table 5: Forced-route evaluation of RAMoEA-QA under expert collapse. We report MacroF1 (discriminative) / MAE (regression) by dataset and question type. **Full** is the fully routed model.

| Dataset | QT | Forced routing | | | | |
|-------------------|---------------------|----------------|------|---------|------|------|
| | | operaCT | | operaGT | | Full |
| | | L1 | L2 | L1 | L2 | |
| KAUH | SV | 0.75 | 0.75 | 1.00 | 1.00 | 1.00 |
| | OE | 0.33 | 0.33 | 0.50 | 0.44 | 0.33 |
| | MC | 0.33 | 0.33 | 0.44 | 0.50 | 0.38 |
| CoughVID | SV | 0.50 | 0.55 | 0.91 | 0.88 | 0.77 |
| | OE | 0.16 | 0.16 | 0.16 | 0.00 | 0.00 |
| | MC | 0.33 | 0.44 | 0.50 | 0.50 | 0.61 |
| ICBHI | SV | 0.75 | 0.75 | 1.00 | 1.00 | 0.71 |
| | OE | 0.31 | 0.25 | 0.25 | 0.25 | 0.43 |
| | MC | 0.50 | 0.50 | 0.50 | 0.50 | 0.43 |
| Resp.@TR | SV | 0.65 | 0.70 | 0.60 | 0.50 | 0.57 |
| | OE | 1.00 | 1.00 | 1.00 | 1.00 | 1.00 |
| | MC | 1.00 | 1.00 | 1.00 | 1.00 | 1.00 |
| Coswara | SV | 0.73 | 0.53 | 0.92 | 0.90 | 0.85 |
| MM Lung | OE (\downarrow) | 3.15 | 2.42 | 2.42 | 3.61 | 2.29 |
| Reg. Avg. | OE (\downarrow) | 3.15 | 2.42 | 4.15 | 3.62 | 2.29 |
| Disc. Avg. | ALL | 0.54 | 0.49 | 0.73 | 0.71 | 0.67 |

Our two-stage routing consistently yields the lowest MAE and remains competitive on discriminative tasks. By selectively leveraging expert-adaptor pairs, the router balances performance across datasets; for instance, it selects the high-performing OPERA-GT/L1 path for 88% of KAUH samples. Crucially, sample-level routing can outperform even the best fixed path, as demonstrated by the superior regression results on the MM Lung dataset. In nearly all dataset-question-type combinations, the full model with routing is either the best option or a strong compromise among forced paths.

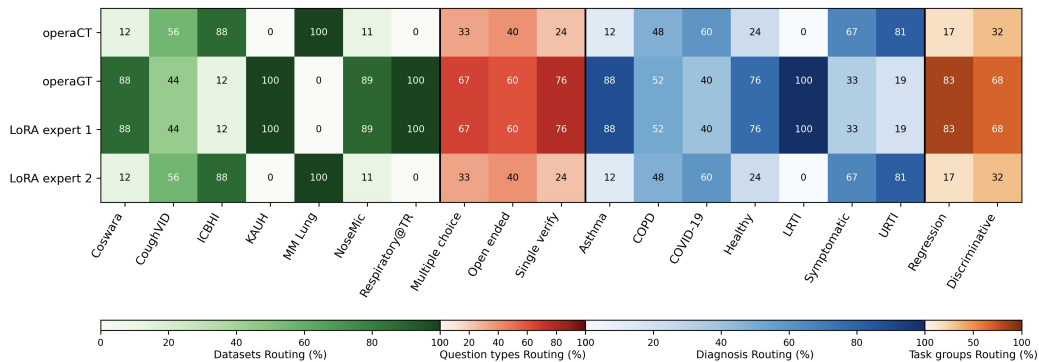


Figure 3: Unified routing heatmap across datasets, question formats, and diagnosis categories. Columns are grouped into Datasets (green), Question types (red), Diagnosis labels (blue), and Tasks (orange), while rows correspond to the four experts (operaCT, operaGT, LoRA expert 1, LoRA expert 2).

6. Discussion

We presented **RAMoEA-QA**, a hierarchical and modular model for respiratory audio question answering built around a two-stage conditional specialization scheme: an *Audio Mixture-of-Experts (Audio-MoE)* selects one frozen audio encoder expert per example, and a *Language Mixture-of-Adapters (MoA)* selects one LoRA-specialized language expert on top of a shared frozen LLM, with both decisions made by lightweight routers. The central empirical takeaway is that this *two-stage routing* (audio-expert selection followed by LoRA-adaptor selection) improves accuracy and robustness across heterogeneous question formats and task families, with the clearest gains on diagnosis-style questions where the model benefits from both acoustic diversity and language specialization.

Importantly, RAMoEA-QA also generalizes better than non-specialized baselines: without modifying the frozen backbones, it transfers more reliably to new datasets, recording conditions, and previously unseen task formulations. Our evaluation spans both *discriminative* (classification/decision) and *regression* question families, and we observe consistent benefits across these supervision types.

Future directions include exploiting *router uncertainty* as a confidence signal for *selective answering* (abstention) and studying how the pro-

posed architecture scales with larger backbones, more experts, and additional data.

References

- Asma Ben Abacha, Sadid A Hasan, Vivek V Datla, Joey Liu, and Henning Muller. VQA-Med: Overview of the Medical Visual Question Answering Task at ImageCLEF 2019.
- Gokhan Altan, Yakup Kutlu, Yusuf Garbi, Adnan Ozhan Pekmezci, and Serkan Nural. Multimedia respiratory database (respiratory-database@tr): Auscultation sounds and chest x-rays, 2021. URL <https://arxiv.org/abs/2101.10946>.
- Anthropic. Advancing claude in healthcare and the life sciences. <https://www.anthropic.com/news/healthcare-life-sciences>, January 2026. Accessed 2026-02-01.
- Gaia A. Bertolino, Yuwei Zang, Tong Xia, Domenico Talia, and Cecilia Mascolo. Ra-qa: Towards respiratory audio-based health question answering. February 2026. doi: 10.5281/zenodo.18489541. URL <https://zenodo.org/records/18489541>.
- Debarpan Bhattacharya, Neeraj Kumar Sharma, Debottam Dutta, Srikanth Raj Chetupalli, Pravin Mote, Sriram Ganapathy, C. Chandrakiran, Sahiti Nori, K. K. Suhail, Sadhana

- Gonuguntla, and Murali Alagesan. Coswara: A respiratory sounds and symptoms dataset for remote screening of SARS-CoV-2 infection. *Scientific Data*, 10(1):397, June 2023. ISSN 2052-4463. doi: 10.1038/s41597-023-02266-0. URL <https://www.nature.com/articles/s41597-023-02266-0>.
- Eric L. Buehler and Markus J. Buehler. X-lora: Mixture of low-rank adapter experts, a flexible framework for large language models with applications in protein mechanics and molecular design. (arXiv:2402.07148), March 2024. doi: 10.48550/arXiv.2402.07148. URL <http://arxiv.org/abs/2402.07148>. arXiv:2402.07148 [cond-mat].
- Kayla-Jade Butkow, Ting Dang, Andrea Ferlini, Dong Ma, Yang Liu, and Cecilia Mascolo. An evaluation of heart rate monitoring with in-ear microphones under motion. *Pervasive and Mobile Computing*, 100:101913, 2024. ISSN 1574-1192. doi: <https://doi.org/10.1016/j.pmcj.2024.101913>. URL <https://www.sciencedirect.com/science/article/pii/S1574119224000397>.
- Yunfei Chu, Jin Xu, Xiaohuan Zhou, Qian Yang, Shiliang Zhang, Zhijie Yan, Chang Zhou, and Jingren Zhou. Qwen-Audio: Advancing Universal Audio Understanding via Unified Large-Scale Audio-Language Models, December 2023. URL <http://arxiv.org/abs/2311.07919>. Issue: arXiv:2311.07919 arXiv:2311.07919 [eess].
- Harry Coppock, George Nicholson, Ivan Kiskin, Vasiliki Koutra, Kieran Baker, Jobie Budd, Richard Payne, Emma Karoune, David Hurley, Alexander Titcomb, Sabrina Egglestone, Ana Tendero Cañadas, Lorraine Butler, Radka Jersakova, Jonathon Mellor, Selina Patel, Tracey Thornley, Peter Diggle, Sylvia Richardson, Josef Packham, Björn W. Schuller, Davide Pigoli, Steven Gilmour, Stephen Roberts, and Chris Holmes. Audio-based ai classifiers show no evidence of improved covid-19 screening over simple symptoms checkers, 2023. URL <https://arxiv.org/abs/2212.08570>.
- Nilaksh Das, Saket Dingliwal, Srikanth Ronanki, Rohit Paturi, Zhaocheng Huang, Prashant Mathur, Jie Yuan, Dhanush Bekal, Xing Niu, Sai Muralidhar Jayanthi, Xilai Li, Karel Mundnich, Monica Sunkara, Sundararajan Srinivasan, Kyu J. Han, and Katrin Kirchhoff. SpeechVerse: A Large-scale Generalizable Audio Language Model, May 2024. URL <http://arxiv.org/abs/2405.08295>. Issue: arXiv:2405.08295 arXiv: 2405.08295 [cs].
- Soham Deshmukh, Benjamin Elizalde, Rita Singh, and Huaming Wang. Pengi: An audio language model for audio tasks. (arXiv:2305.11834), January 2024a. doi: 10.48550/arXiv.2305.11834. URL <http://arxiv.org/abs/2305.11834>. arXiv:2305.11834 [eess].
- Soham Deshmukh, Benjamin Elizalde, Rita Singh, and Huaming Wang. Pengi: An Audio Language Model for Audio Tasks, January 2024b. URL <http://arxiv.org/abs/2305.11834>. arXiv:2305.11834 [eess].
- Mohamed Elgendi, Fridolin Haugg, Richard Ribbon Fletcher, John Allen, Hangsik Shin, Aymen Alian, and Carlo Menon. Recommendations for evaluating photoplethysmography-based algorithms for blood pressure assessment. *Communications Medicine*, 4(1):140, 2024. ISSN 2730-664X. doi: 10.1038/s43856-024-00555-2.
- William Fedus, Barret Zoph, and Noam Shazeer. Switch transformers: Scaling to trillion parameter models with simple and efficient sparsity, 2022. URL <https://arxiv.org/abs/2101.03961>.
- Mohammad Fraiwan, Luay Fraiwan, Mohanad Alkhodari, and Omnia Hassanin. Recognition of pulmonary diseases from lung sounds using convolutional neural networks and long short-term memory. *Journal of Ambient Intelligence and Humanized Computing*, 13:4759–4771, 04 2021a. doi: 10.1007/s12652-021-03184-y.
- Mohammad Fraiwan, Luay Fraiwan, Basheer Khassawneh, and Ali Ibnian. A dataset of lung sounds recorded from the chest wall using an electronic stethoscope. *Data in Brief*, 35:106913, 2021b. ISSN 2352-3409. doi: <https://doi.org/10.1016/j.dib.2021.106913>. URL <https://www.sciencedirect.com/science/article/pii/S2352340921001979>.

- Siddhartha Gairola, Francis Tom, Nipun Kwatra, and Mohit Jain. Respirenet: A deep neural network for accurately detecting abnormal lung sounds in limited data setting. In *2021 43rd Annual International Conference of the IEEE Engineering in Medicine & Biology Society (EMBC)*, pages 527–530, 2021. doi: 10.1109/EMBC46164.2021.9630091.
- Sreyan Ghosh, Sonal Kumar, Ashish Seth, Chandra Kiran Reddy Evuru, Utkarsh Tyagi, S Sakshi, Oriol Nieto, Ramani Duraiswami, and Dinesh Manocha. Gama: A large audio-language model with advanced audio understanding and complex reasoning abilities, 2024. URL <https://arxiv.org/abs/2406.11768>.
- Yuan Gong, Hongyin Luo, Alexander H. Liu, Leonid Karlinsky, and James Glass. Listen, think, and understand, 2024. URL <https://arxiv.org/abs/2305.10790>.
- Google AI. Health ai. <https://ai.google/health/>, n.d. Accessed 2026-02-01.
- Jiang Guo, Darsh J. Shah, and Regina Barzilay. Multi-source domain adaptation with mixture of experts. (arXiv:1809.02256), October 2018. doi: 10.48550/arXiv.1809.02256. URL <http://arxiv.org/abs/1809.02256>. arXiv:1809.02256 [cs].
- Edward J. Hu, Yelong Shen, Phillip Wallis, Zeyuan Allen-Zhu, Yuanzhi Li, Shean Wang, Lu Wang, and Weizhu Chen. Lora: Low-rank adaptation of large language models, 2021. URL <https://arxiv.org/abs/2106.09685>.
- Yutao Hu, Tianbin Li, Quanfeng Lu, Wenqi Shao, Junjun He, Yu Qiao, and Ping Luo. OmniMedVQA: A New Large-Scale Comprehensive Evaluation Benchmark for Medical LLM, April 2024. URL <http://arxiv.org/abs/2402.09181>. arXiv:2402.09181 [eess].
- Rongjie Huang, Mingze Li, Dongchao Yang, Jiantong Shi, Xuankai Chang, Zhenhui Ye, Yuning Wu, Zhiqing Hong, Jiawei Huang, Jinglin Liu, Yi Ren, Zhou Zhao, and Shinji Watanabe. Audiogpt: Understanding and generating speech, music, sound, and talking head, 2023. URL <https://arxiv.org/abs/2304.12995>.
- Robert Jacobs, Michael Jordan, Steven Nowlan, and Geoffrey Hinton. Adaptive mixtures of local experts. *Neural Computation*, 3:79–87, 03 1991. doi: 10.1162/neco.1991.3.1.79.
- Qiao Jin, Bhuwan Dhingra, Zhengping Liu, William W. Cohen, and Xinghua Lu. PubMedQA: A Dataset for Biomedical Research Question Answering, September 2019. URL <http://arxiv.org/abs/1909.06146>. Issue: arXiv:1909.06146 arXiv: 1909.06146 [cs].
- Wassim Labaki and Meilan Han. Chronic respiratory diseases: a global view. *The Lancet Respiratory Medicine*, 8:531–533, 06 2020. doi: 10.1016/S2213-2600(20)30157-0.
- Gyubok Lee, Hyeonji Hwang, Seongsu Bae, Yeonsu Kwon, Woncheol Shin, Seongjun Yang, Minjoon Seo, Jong-Yeup Kim, and Edward Choi. Ehrsql: A practical text-to-sql benchmark for electronic health records, 2023. URL <https://arxiv.org/abs/2301.07695>.
- Gyuseong Lee, Wooseok Jang, Jinhyeon Kim, Jaewoo Jung, and Seungryong Kim. Domain generalization using large pretrained models with mixture-of-adapters. (arXiv:2310.11031), December 2024. doi: 10.48550/arXiv.2310.11031. URL <http://arxiv.org/abs/2310.11031>. arXiv:2310.11031 [cs].
- Dmitry Lepikhin, HyoukJoong Lee, Yuanzhong Xu, Dehao Chen, Orhan Firat, Yanping Huang, Maxim Krikun, Noam Shazeer, and Zhifeng Chen. Gshard: Scaling giant models with conditional computation and automatic sharding, 2020. URL <https://arxiv.org/abs/2006.16668>.
- Mohammed Mosuily, Lindsay Welch, and Jagmohan Chauhan. Mmlung: Moving closer to practical lung health estimation using smartphones. In *Interspeech 2023*, pages 2333–2337, 2023. doi: 10.21437/Interspeech.2023-721.
- Sai Munikoti, Ian Stewart, Sameera Horawalavithana, Henry Kvinge, Tegan Emerson, Sandra E. Thompson, and Karl Pazdernik. Generalist multimodal ai: A review of architectures, challenges and opportunities, 2024.
- Vincent Nguyen, Sarvnaz Karimi, Maciej Rybinski, and Zhenchang Xing. MedRedQA for Medical Consumer Question Answering: Dataset,

- Tasks, and Neural Baselines. In *Proceedings of the 13th International Joint Conference on Natural Language Processing and the 3rd Conference of the Asia-Pacific Chapter of the Association for Computational Linguistics (Volume 1: Long Papers)*, pages 629–648, Nusa Dua, Bali, 2023. Association for Computational Linguistics. doi: 10.18653/v1/2023.ijcnlp-main.42. URL <https://aclanthology.org/2023.ijcnlp-main.42>.
- Jungwoo Oh, Gyubok Lee, Seongsu Bae, Joonmyoung Kwon, and Edward Choi. ECG-QA: A Comprehensive Question Answering Dataset Combined With Electrocardiogram, October 2023. URL <http://arxiv.org/abs/2306.15681>. Issue: arXiv:2306.15681 arXiv: 2306.15681 [q-bio].
- OpenAI. Introducing chatgpt health. <https://openai.com/index/introducing-chatgpt-health/>, January 2026. Accessed 2026-02-01.
- Lara Orlandic, Tomas Teijeiro, and David Atenza. The COUGHVID crowdsourcing dataset, a corpus for the study of large-scale cough analysis algorithms. *Scientific Data*, 8(1):156, June 2021. ISSN 2052-4463. doi: 10.1038/s41597-021-00937-4. URL <https://doi.org/10.1038/s41597-021-00937-4>.
- Eoin O’Brien, Bernard Waeber, Gianfranco Parati, Jan Staessen, and Martin G Myers. Blood pressure measuring devices: recommendations of the european society of hypertension. *BMJ: British Medical Journal*, 322(7285): 531–536, March 2001. ISSN 0959-8138. doi: 10.1136/bmj.322.7285.531.
- Anusri Pampari, Preethi Raghavan, Jennifer Liang, and Jian Peng. emrqa: A large corpus for question answering on electronic medical records, 2018. URL <https://arxiv.org/abs/1809.00732>.
- Jonas Pfeiffer, Aishwarya Kamath, Andreas Rücklé, Kyunghyun Cho, and Iryna Gurevych. Adapterfusion: Non-destructive task composition for transfer learning. In Paola Merlo, Jorg Tiedemann, and Reut Tsarfaty, editors, *Proceedings of the 16th Conference of the European Chapter of the Association for Computational Linguistics: Main Volume*, page 487–503, Online, April 2021. Association for Computational Linguistics. doi: 10.18653/v1/2021.eacl-main.39. URL <https://aclanthology.org/2021.eacl-main.39/>.
- Sandra Reichert, Raymond Gass, Christian Brandt, and Emmanuel Andrès. Analysis of respiratory sounds: state of the art. *Clin. Med. Circ. Respirat. Pulm. Med.*, 2:45–58, May 2008.
- Bruno M Rocha, Dimitris Filos, Luís Mendes, Gorkem Serbes, Sezer Ulukaya, Yasemin P Kahya, Nikša Jakovljevic, Tatjana L Turukalo, Ioannis M Vogiatzis, Eleni Perantoni, Evangelos Kaimakamis, Pantelis Natsiavas, Ana Oliveira, Cristina Jácome, Alda Marques, Nicos Maglaveras, Rui Pedro Paiva, Ioanna Chouvarda, and Paulo de Carvalho. An open access database for the evaluation of respiratory sound classification algorithms. *Physiological Measurement*, 40(3): 035001, March 2019. doi: 10.1088/1361-6579/ab03ea. URL <https://dx.doi.org/10.1088/1361-6579/ab03ea>. Publisher: IOP Publishing.
- Karan Singhal, Shekoofeh Azizi, Tao Tu, S. Sara Mahdavi, Jason Wei, Hyung Won Chung, Nathan Scales, Ajay Tanwani, Heather Cole-Lewis, Stephen Pfohl, Perry Payne, Martin Seneviratne, Paul Gamble, Chris Kelly, Nathaneal Scharli, Aakanksha Chowdhery, Philip Mansfield, Blaise Aguerre y Arcas, Dale Webster, Greg S. Corrado, Yossi Matias, Katherine Chou, Juraj Gottweis, Nenad Tomasev, Yun Liu, Alvin Rajkomar, Joelle Barral, Christopher Sementurs, Alan Karthikesalingam, and Vivek Natarajan. Large language models encode clinical knowledge, 2022. URL <https://arxiv.org/abs/2212.13138>.
- Anssi Sovijärvi, F. Dalmasso, J. Vanderschoot, Leo Malmberg, G. Righini, and S.A.T. Stone-man. Definition of terms for applications of respiratory sounds. *Eur Respir Rev*, 10, 11 1999.
- Arpan Srivastava, Sonakshi Jain, Ryan Miranda, Shruti Patil, Sharnil Pandya, and Ketan Kotecha. Deep learning based respiratory sound analysis for detection of chronic obstructive

- tive pulmonary disease. *PeerJ Computer Science*, 7, 02 2021. doi: 10.7717/peerj-cs.369.
- George Tsatsaronis, Georgios Balikas, Prodromos Malakasiotis, Ioannis Partalas, Matthias Zschunke, Michael R. Alvers, Dirk Weisenborn, Anastasia Krithara, Sergios Petridis, Dimitris Polychronopoulos, Yannis Almirantis, John Pavlopoulos, Nicolas Baskiotis, Patrick Gallinari, Thierry Artières, Axel-Cyrille Ngonga Ngomo, Norman Heino, Eric Gaussier, Liliana Barrio-Alvers, Michael Schroeder, Ion Androutopoulos, and Georgios Paliouras. An overview of the bioasq large-scale biomedical semantic indexing and question answering competition. *BMC Bioinformatics*, 16(1):138, April 2015. ISSN 1471-2105. doi: 10.1186/s12859-015-0564-6.
- Ping Wang, Tian Shi, and Chandan K. Reddy. Text-to-sql generation for question answering on electronic medical records, 2020. URL <https://arxiv.org/abs/1908.01839>.
- Renzhi Wang and Piji Li. Memoe: Enhancing model editing with mixture of experts adapters. (arXiv:2405.19086), 2024. doi: 10.48550/arXiv.2405.19086. URL <http://arxiv.org/abs/2405.19086>. arXiv:2405.19086 [cs].
- Tsai-Ning Wang, Lin-Lin Chen, Neil Zeghidour, and Aaqib Saeed. Careaqa: A cardiac and respiratory audio question answering model for open-ended diagnostic reasoning. (arXiv:2505.01199), 2025. doi: 10.48550/arXiv.2505.01199. URL <http://arxiv.org/abs/2505.01199>. arXiv:2505.01199 [cs].
- Shengqiong Wu, Hao Fei, Leigang Qu, Wei Ji, and Tat-Seng Chua. Next-gpt: Any-to-any multimodal llm, 2024a. URL <https://arxiv.org/abs/2309.05519>.
- Xun Wu, Shaohan Huang, and Furu Wei. Mixture of lora experts. (arXiv:2404.13628), April 2024b. doi: 10.48550/arXiv.2404.13628. URL <http://arxiv.org/abs/2404.13628>. arXiv:2404.13628 [cs].
- Tianyi Zhang, Varsha Kishore, Felix Wu, Kilian Q. Weinberger, and Yoav Artzi. BERTscore: Evaluating text generation with bert, 2020. URL <https://arxiv.org/abs/1904.09675>.
- Yuwei Zhang, Tong Xia, Jing Han, Yu Wu, Georgios Rizos, Yang Liu, Mohammed Mosuly, Jagmohan Chauhan, and Cecilia Mascolo. Towards open respiratory acoustic foundation models: Pretraining and benchmarking, 2024. URL <https://arxiv.org/abs/2406.16148>.

Appendix A. Datasets overview

The RA-QA collection is built upon 11 distinct datasets, each contributing to the overall diversity and richness of the resource (dataset availability is reported in Table 6). This section provides a more detailed overview of these datasets. Each dataset comprises two core components: a metadata file and a corresponding audio set. The metadata encompasses structured clinical and contextual information, while the audio data consists of respiratory-related recordings. All audio recordings are fully anonymized and the associated metadata have been carefully curated to exclude any personally identifiable information or inappropriate content, ensuring compliance with ethical standards and data protection regulations. This unified structure supports consistent integration and facilitates downstream research tasks. Following this introduction, a more detailed description is provided for each dataset from the RA-QA collection used in this paper. Table 7 reports the number of recordings and QA pairs used per dataset, split, modality, and task family within training.

UK COVID-19 (Coppock et al., 2023). The UK COVID-19 Vocal Audio Dataset is designed for training and evaluating machine learning models to classify SARS-CoV-2 infection status and associated respiratory symptoms using vocal audio. The dataset was collected by the UK Health Security Agency from March 2021 to March 2022, during the prevalence of the Alpha and Delta SARS-CoV-2 variants, as well as some Omicron sublineages. Participants were recruited through the national Test and Trace programme and the REACT-1 survey. Audio recordings of voluntary coughs and exhalations were gathered through the ‘Speak up to help beat coronavirus’ digital survey, alongside demographic data, self-reported symptoms and respiratory conditions (see

Table 6: Dataset Availability: The ICBHI and HF Lung datasets are sourced from multiple origins; please refer to the detailed description in the text below. The MMLung and NoseMic datasets are available upon request. The specific licensing terms are outlined in the Data Transfer Agreement (DTA).

| Dataset | Source | Access | License |
|----------------|--------|--|---------------------------|
| UK COVID-19 | IC | https://zenodo.org/records/10043978 | OGL 3.0 |
| CoughVID | EPFL | https://zenodo.org/records/4048312 | CC BY 4.0 |
| ICBHI | * | https://bhichallenge.med.auth.gr | CC0 |
| HF Lung | * | https://gitlab.com/techsupportHF/HF_Lung_V1 https://gitlab.com/techsupportHF/HF_Lung_V1_IP | CC BY 4.0 CC BY-NC 4.0 |
| Coswara | IISc | https://github.com/iiscleap/Coswara-Data | CC BY 4.0 |
| KAUH | KAUH | https://data.mendeley.com/datasets/jwyy9np4gv/3 | CC BY 4.0 |
| Respiratory@TR | ITU | https://data.mendeley.com/datasets/p9z4h98s6j/1 | CC BY 4.0 |
| MMLung | UoS | https://github.com/MohammedMosuily/mmlung | Custom license |
| NoseMic | UoC | https://github.com/evelyn0414/OPERA/tree/main/datasets/nosemic | Custom license |

Table 7: Statistics of the RA-QA collection used in the training. For each dataset we report the task family, target task, audio modalities, and the number of derived QA pairs per split (Train/Val/Test). An asterisk (*) denotes datasets where the diagnosis task is available only in the single-verify format.

| Task Family | Dataset | Task | Modalities | QA N (T/V/Te) |
|----------------|----------------|--|-------------------------------------|---------------|
| Discriminative | Coswara | Asthma * | Deep and shallow breathing | 204 / 64 / 64 |
| | COUGHVID | Diagnosis (Healthy, Symptomatic, Covid-19) | Coughing | 225 / 45 / 45 |
| | ICBHI | Diagnosis (URTI, COPD) | Four clinical recording devices | 423 / 32 / 32 |
| | KAUH | Diagnosis (Healthy, LRTI, COPD) | 6 sound types and 7 chest positions | 225 / 45 / 45 |
| | Respiratory@TR | COPD Severity | 11 recording positions | 210 / 70 / 70 |
| Regression | MM-Lung | Spirometry (FEV1) | Deep breathing | 32 / 4 / 4 |
| | MM-Lung | Spirometry (FVC) | Deep breathing | 32 / 4 / 4 |
| | Nosemic | Respiratory rate | Before and after running | 50 / 9 / 9 |

Figure 4). These recordings were linked to SARS-CoV-2 test results, although speech recordings are not included in the open access version of the dataset and were not used in this study. The study was approved by The National Statistician’s Data Ethics Advisory Committee (reference NSDEC(21)01), the Cambridge South NHS Research Ethics Committee (reference 21/EE/0036) and the Nottingham NHS Research Ethics Committee (reference 21/EM/0067). Informed consent was obtained from all participants.

COUGHVID (Orlandic et al., 2021) The COUGHVID dataset consists of over 25,000 crowdsourced cough recordings, collected from a diverse group of participants across different ages, genders, geographic locations, and COVID-19 statuses (see Figure 5). All data collection and annotation processes adhered to the relevant ethical guidelines, with informed consent obtained from all participants who submitted their cough recordings and associated metadata.

ICBHI (Rocha et al., 2019) The ICBHI Respiratory Sound Database includes audio samples collected by two independent research teams from different countries over several years. Ethical approval was granted by the relevant ethics committees of the respective institutions. The majority of the database comprises audio samples recorded by the School of Health Sciences, University of Aveiro (ESSUA) research team at the Respiratory Research and Rehabilitation Laboratory (Lab3R) in Aveiro, Portugal and Hospital Infante D. Pedro. The second team, from Aristotle University of Thessaloniki (AUTH) and the University of Coimbra (UC), collected respiratory sounds at Papanikolaou General Hospital in Thessaloniki and the General Hospital of Imathia (Health Unit of Naousa), Greece. The database contains a total of 5.5 hours of recordings across 920 annotated audio samples from 126 subjects (see Figure 6).

MM Lung (Mosuily et al., 2023): The MMLung dataset was collected from 40 participants (20 male, 20 female) aged 18 to 85 years, all of whom are English speakers from the UK. Among the participants, 12 were healthy, while the others

included seven self-reported COPD patients, seven self-reported asthma patients, and 14 individuals with other long-term conditions. Ethical approval for this study was granted by the University of Southampton. Data were gathered using three devices: a Google Pixel 6 smartphone with a custom app for data collection and an Easy on-PC ultrasonic spirometer from nnd Medical Technologies. The audio data was collected in stereo mode at a sampling rate of 44,100 Hz, saved in WAV format and recorded in a quiet room to ensure optimal conditions. The data collection included four audio modalities: cough, vowels, mobile spirometry and speech, through a series of tasks performed in a single session by each participant. For this paper, only the deep breath and the vowel sound of ‘o’ are included (see Figure 7). Ground truth data were obtained using a medical-grade spirometer, with measurements taken by a healthcare professional according to European Respiratory Society (ATS/ERS) clinical standards. However, it is important to note that objective measurements can be subject to individual effort, which may introduce some errors (e.g., effort-dependent blows). This dataset is available upon request.

Coswara (Bhattacharya et al., 2023) The Coswara dataset consists of respiratory sounds recorded between April 2020 and February 2022 from 2,635 individuals, including 1,819 SARS-CoV-2 negative, 674 positive and 142 recovered participants. The dataset includes nine categories of respiratory sounds related to breathing, coughing, and speech. Metadata accompanying the recordings contains demographic details such as age, gender and geographic location, as well as health-related information including symptoms, pre-existing respiratory conditions, comorbidities and SARS-CoV-2 test status (see Figure 8). The data collection was approved by the Institutional Human Ethics Committee at the Indian Institute of Science, Bangalore. Informed consent was obtained from all participants who uploaded their data and the collected data was anonymized to exclude personally identifiable information.

KAUH (Fraivan et al., 2021b) The KAUH dataset includes audio recordings of lung sounds from patients with seven different respiratory

conditions: asthma, heart failure, pneumonia, bronchitis, pleural effusion, lung fibrosis and chronic obstructive pulmonary disease (COPD), as well as normal breathing sounds (see Figure 9). The recordings were made using an electronic stethoscope, with the chest wall examined at various points by a specialist physician. Each sound was recorded three times with different frequency filters to highlight specific bodily sounds. This dataset is valuable for the development of automated systems designed to detect pulmonary diseases or classify lung sounds. All participants (or their parents in the case of minors), provided written informed consent for their inclusion in the study and the sharing of their data. The study was approved by the Institutional Review Board at King Abdullah University Hospital and Jordan University of Science and Technology (Ref. 91/136/2020). Data collection adhered to all relevant ethical guidelines and regulations and the authors have the right to share the data publicly.

NoseMic (Butkow et al., 2024) The NoseMic dataset is a subset of data collected for a respiratory rate estimation project. The audio recordings were captured using microphones positioned close to the participants’ noses, while respiratory dynamics were measured using a Zephyr pressure sensor on the chest. Data collection took place in a stationary environment, both before and after physical exercise. A total of 21 participants were involved in the study, with data from some participants excluded due to poor sensing quality. The benchmark includes audio recordings from before and after running, with each recording segmented into 30-second windows that overlap by 15 seconds. The average respiratory rate for each window was used as the ground truth.

Respiratory@TR (Altan et al., 2021) The Respiratory@TR dataset contains lung sounds recorded from both the left and right sides of the posterior and anterior chest wall, as well as the back, using two digital stethoscopes at Antakya State Hospital. In addition to the lung sound recordings, the dataset includes chest X-rays, pulmonary function test (PFT) variables, spirometric curves and the St. George Respiratory Questionnaire (SGRQ-C) as multimedia

and clinical functional analysis data. The lung sounds were captured across 12 channels, focusing on the upper, middle and lower lung regions, as well as the costophrenic angles on both the posterior and anterior chest sides. The recordings were validated and labeled by two pulmonologists, who assessed the chest X-rays, PFT results and auscultation sounds of the subjects. The labels correspond to five levels of COPD severity (COPD0, COPD1, COPD2, COPD3, COPD4). The dataset was released by Iskenderun Technical University, Turkey. Participation was voluntary and patients, aged 38 to 68, were selected from various occupational groups, socioeconomic backgrounds and genders to ensure a diverse representation of the disorders.

Appendix B. Metrics overview

We follow the RA-QA evaluation protocol (Bertolino et al., 2026) and report both *text-level* and *task-level* metrics to separately capture (i) how well the model matches the reference form and semantics, and (ii) whether it predicts the correct clinical label or value. Text-level metrics are computed directly between the generated answer and the reference after standard normalization, while task-level metrics operate on an *extracted* label/value from the output and therefore ignore any additional explanatory context.

B.1. Metrics for discriminative tasks.

We group discriminative evaluation into *response form* metrics and *label-correctness* metrics.

B.1.1. RESPONSE FORM METRICS.

These metrics assess surface fidelity and semantic similarity of the generated answer:

- **Exact Match (EM)** evaluates whether the normalized predicted response matches the normalized reference string exactly (strict match). EM is informative for structured outputs but can underestimate performance for valid paraphrases.
- **TokenF1** measures token-level overlap between prediction and reference using the harmonic mean of token precision and token recall. TokenF1 rewards partial matches and is less brittle than EM.

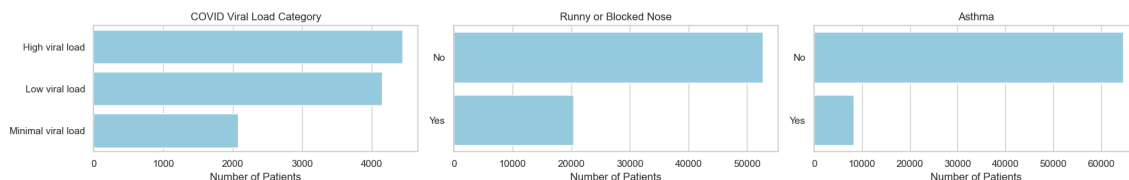


Figure 4: The figure shows label distributions for viral load categories (multiclass), as well as binary labels for symptoms such as runny or blocked nose and conditions like asthma from the UK COVID-19 dataset. As with other datasets used in this work, these labels are highly imbalanced and require preprocessing and reduction strategies to ensure meaningful training and evaluation.

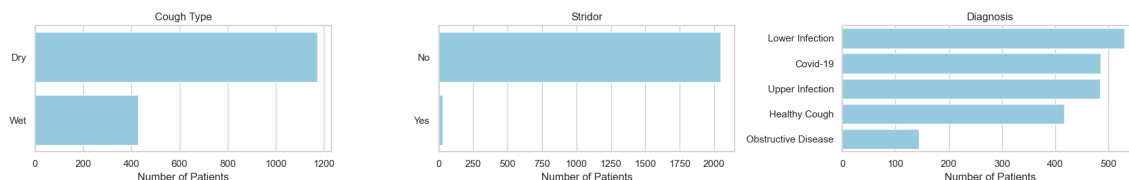


Figure 5: Label distributions from the CoughVid dataset, illustrating examples of audio-related attributes such as cough type, presence of stridor and associated diagnoses. This highlights that, beyond clinical metadata, some datasets also include perceptual or acoustic labels (e.g., wheezes, stridors), which are directly linked to the audio signal and can support more fine-grained sound analysis.

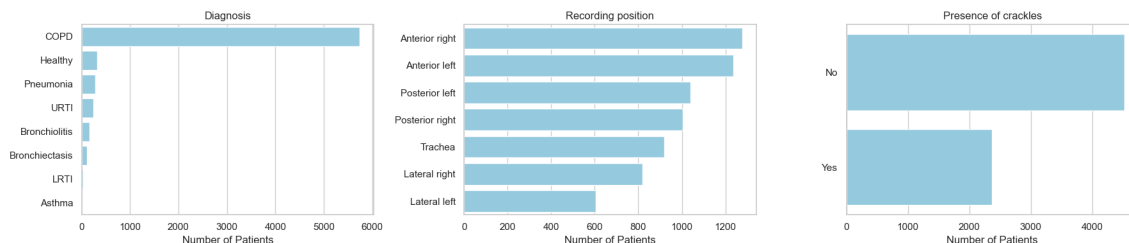


Figure 6: Label distributions from the ICBHI dataset, showing the annotated diagnosis categories, presence of crackles and recording positions (e.g., trachea, anterior left, posterior right). This exemplifies how some datasets provide detailed contextual metadata, such as auscultation position, which can be crucial for interpreting respiratory sounds and modeling location-sensitive acoustic features.

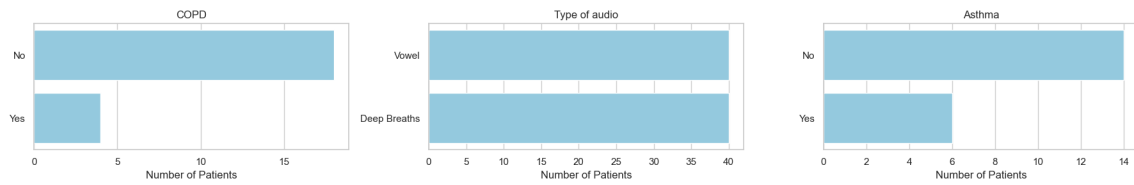


Figure 7: The figure illustrates key characteristics from the MM Lung dataset. The Type of Audio distinguishes between different types of respiratory recordings, such as vowel phonation and deep breathing, which capture varied aspects of lung sound dynamics.

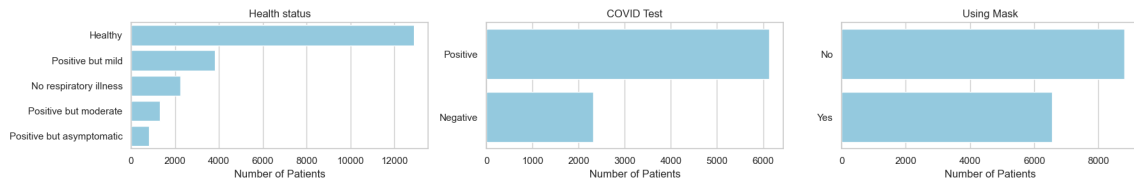


Figure 8: The figure presents the distribution from the Coswara dataset of the selected attributes health status, COVID test result and mask usage at the time of recording. The Health Status attribute distinguishes between healthy individuals and COVID-19 positive cases with varying symptom severity, categorized as asymptomatic, mild or moderate.

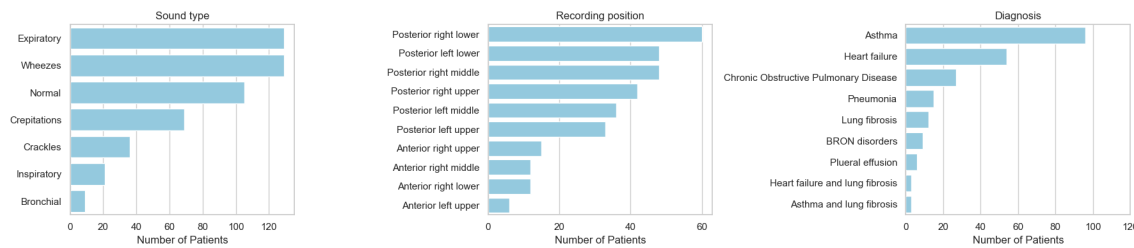


Figure 9: The figure displays key attributes of the KAUH dataset: sound type, recording position and diagnosis. The Sound Type plot shows the presence of multiple annotated labels per recording.

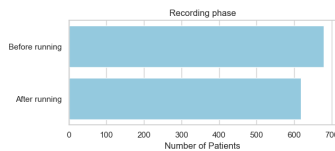


Figure 10: The plots illustrate the recording phase attribute distribution from the NoseMic dataset. This captures whether the respiratory sounds were recorded before or after physical exertion (e.g., running), which is important for evaluating exertion-induced changes in breathing patterns.

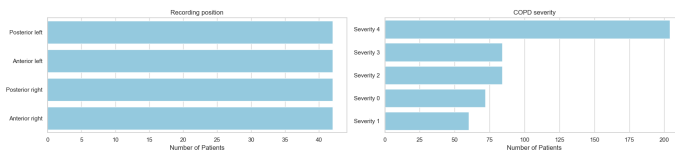


Figure 11: The plots illustrate two key attributes from the Respiratory@TR dataset: recording position and COPD severity. The recording position captures the recording point while the COPD Severity is scored on a scale from 0 (no COPD) to 4 (very severe), providing clinically relevant gradation to analyze how disease progression correlates with acoustic features in the recordings.

- **METEOR** measures lexical alignment between prediction and reference, designed to be robust to minor morphological variation and alternate word forms via flexible word-level matching.
- **BERTScore** (Zhang et al., 2020) measures semantic similarity by computing cosine similarity between contextual token embeddings from a pre-trained BERT model and aggregating alignment scores across tokens. It provides a semantic view that is less sensitive to paraphrasing than n-gram overlap metrics.

Together, EM/TokenF1 emphasize surface-form fidelity, METEOR captures word-level matching under small lexical variations, and BERTScore provides a semantics-oriented complement for open-ended answers.

B.1.2. LABEL-CORRECTNESS METRICS.

For diagnosis-style questions, we evaluate *label correctness* by extracting the target label from

the model output and comparing it to the ground truth, ignoring extra answer context. For open-ended and multiple-choice questions, we parse the generated text to recover the predicted diagnosis label (e.g., by normalizing case/punctuation and matching against the dataset label set), whereas for single-verify questions we parse the output into {Yes, No}. We then compute:

- **Accuracy** as the fraction of examples whose extracted label matches the ground truth. While interpretable, accuracy can be misleading under class imbalance.
- **Macro F1-score (MacroF1)** as the unweighted mean of per-class F1-scores, where each class contributes equally. MacroF1 is robust to imbalance and reflects the precision-recall trade-off, which is important in clinical settings where both missed cases (false negatives) and false alarms (false positives) carry cost.

We emphasize **MacroF1** as the primary discriminative metric due to its robustness to skewed la-

bel distributions and its balanced accounting of false positives and false negatives.

B.2. Metrics for regression tasks.

For numeric targets, we treat the model output as free-form text and *parse* a scalar prediction by extracting the first valid numeric value in the generated answer (if present). We then compare this extracted value \hat{y} to the ground-truth target y and compute error metrics over successfully parsed examples (lower is better). Concretely, we report:

- **Mean Absolute Error (MAE):** $\text{MAE} = \frac{1}{N} \sum_{i=1}^N |\hat{y}_i - y_i|$, which measures the average absolute deviation and is less sensitive to occasional outliers.
- **Root Mean Squared Error (RMSE):** $\text{RMSE} = \sqrt{\frac{1}{N} \sum_{i=1}^N (\hat{y}_i - y_i)^2}$, which penalizes larger errors more strongly and is therefore sensitive to rare but severe misestimates.

Because regression evaluation depends on successful numeric extraction from free-form generations, we additionally report **parsing coverage**, i.e., the fraction of test instances for which numeric extraction succeeds. Unless otherwise stated, MAE/RMSE are computed on the subset of examples with valid numeric parses.

Appendix C. Routing and conditioning details

Audio-MoE routing vector. We denote the Audio-MoE routing vector by $\mathbf{r}_a \in \mathbb{R}^{d_r}$ and instantiate the router-input policy as:

$$\mathbf{r}_a \in \{\mathbf{z}_{\text{audio}}^a, \mathbf{z}_{\text{question}}^a, \mathbf{z}_{\text{fused}}^a\}, \quad (2)$$

where $\mathbf{z}_{\text{audio}}^a$ is obtained from a shallow spectrogram proxy extractor \mathcal{F} and pooling, $\mathbf{z}_{\text{question}}^a$ is a pooled question embedding projected to d_r , and $\mathbf{z}_{\text{fused}}^a$ is computed via lightweight cross-attention between question tokens and proxy audio tokens. The router MLP produces logits over N_a experts and selects a single expert via straight-through Gumbel-Softmax in training and argmax at inference.

Audio expert encoding and alignment. Given the selected expert index e_a , only $\mathcal{E}_{e_a}^a$ encodes the spectrogram to produce $\mathbf{h}_{e_a}^a$, which is aligned to the LLM hidden size d_ℓ with an expert-specific aligner \mathcal{A}_{e_a} :

$$\tilde{\mathbf{h}}_{e_a}^a = \mathcal{A}_{e_a}(\mathbf{h}_{e_a}^a) \in \mathbb{R}^{T_{e_a} \times d_\ell}. \quad (3)$$

Selected audio prefix and LLM input. We inject the aligned audio embeddings as a *selected audio prefix* by concatenating them into the LLM input embeddings:

$$\mathbf{X} = [\mathbf{H}_p; \tilde{\mathbf{h}}_{e_a}^a; \mathbf{H}_{\text{Ans}}; \mathbf{H}_y], \quad (4)$$

where \mathbf{H}_p encodes the prompt/question, \mathbf{H}_{Ans} is an ‘‘Answer:’’ tag, and \mathbf{H}_y are teacher-forced answer embeddings during training.

LoRA-MoA routing vector. Analogously, the MoA routing vector $\mathbf{r}_\ell \in \mathbb{R}^{d_\ell}$ instantiates the same router-input policy at the language stage:

$$\mathbf{r}_\ell \in \{\mathbf{z}_{\text{audio}}^\ell, \mathbf{z}_{\text{question}}^\ell, \mathbf{z}_{\text{fused}}^\ell\}, \quad (5)$$

with $\mathbf{z}_{\text{audio}}^\ell = \text{Pool}(\tilde{\mathbf{h}}_{e_a}^a)$, $\mathbf{z}_{\text{question}}^\ell = \text{Pool}(\mathbf{H}_p)$, and $\mathbf{z}_{\text{fused}}^\ell$ computed by lightweight fusion between prompt and the selected aligned audio embeddings. The adapter router outputs logits over N_ℓ LoRA adapters and selects one adapter via straight-through Gumbel-Softmax (train) and argmax (eval).

Appendix D. Baselines

We compare RAMoEA-QA against two representative baselines: (i) a general-purpose audio-language model used *as-is* (PENGI), and (ii) a domain-specific audio-QA architecture implemented as a *monolithic* (single-path) counterpart to our routed model (CAREQA-STYLE).

D.1. Pengi (general-purpose audio-language model)

PENGI is a general audio-language model originally designed for broad audio captioning and QA-style generation across diverse audio domains (see Figure 12). It formulates a wide range of audio tasks as *audio+text* \rightarrow *text* generation by conditioning a (largely) frozen causal language model on a fixed-length *prefix* built from an audio embedding and a text-prompt embedding, each

mapped through lightweight trainable networks (Deshmukh et al., 2024b). In our experiments, we use PENGU *without additional fine-tuning* on RA-QA: we provide the respiratory recording and question as input and decode answers using the model’s default generation procedures. Because PENGU is not trained for clinically structured respiratory assessment (nor specialized to RA-QA labels, question formats, or respiratory acoustics), it serves as a reference point for the limitations of general multimodal audio-language models when transferred to respiratory clinical QA. This baseline therefore tests how far a strong, task-general audio-language model transfers under dataset, modality, and task shifts.

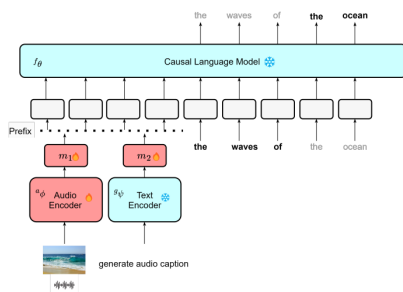


Figure 12: Overview of the Pengi architecture used as a baseline in our experiments.

D.2. CaReAQA-style monolithic audio-QA model

CAREAQA is an audio-language QA framework for cardiac and respiratory diagnostic reasoning that combines an audio encoder with a decoder-only LLM to produce open-ended answers (Wang et al., 2025). Its core design maps audio features into the LLM hidden space via an audio mapper and injects the resulting aligned embeddings as a soft prefix for autoregressive generation. Prior work in this line is typically trained and evaluated primarily in a monolithic setting and on a single question format (open-ended), and does not explicitly analyze conditional specialization mechanisms (e.g., expert routing or format-/intent-dependent pathways) across heterogeneous datasets and question types.

To isolate the effect of *routing* in a controlled comparison, we implement a **monolithic** baseline that mirrors the CAREAQA-style pipeline: (i) a *single* audio encoder processes every spectrogram, (ii) a *single* audio-to-LLM aligner produces aligned audio embeddings, and (iii) a *single* LLM pathway (one adapter (one set of trainable parameters) on a frozen backbone, matching our training recipe) generates the answer from the prompt plus aligned audio prefix. This baseline keeps the multimodal interface (audio-prefix injection and autoregressive objective) comparable to RAMoEA-QA, while forcing all examples through one fixed acoustic representation and one fixed generation behavior.

Appendix E. Further results

This appendix provides the complete breakdown of results for both **discriminative** and **regressive** RA-QA tasks. For discriminative tasks, we report per-dataset performance across question types (Global, Single-verify, Open-ended, and Multiple-choice) using standard classification and string-level metrics (e.g., Accuracy, MacroF1, TokenF1, Exact Match), as well as semantic similarity scores (BERTScore and METEOR). For regressive tasks, we report per-dataset performance for each target variable (e.g., MM Lung: FEV1/FVC; NoseMic: respiratory rate) using error-based metrics (MAE and RMSE).

Tables in this section are organized to facilitate direct comparison **across datasets** and **across question types**, highlighting how performance varies depending on both the underlying data source and the QA formulation.

Table 8: Per-dataset breakdown for in-domain testing (mean \pm std over runs) for the baseline configuration of operaGT on discriminative tasks.

| Metric | Subset | Global | Coswara | CoughVid | ICBHI | KAUH | Respiratory@TR |
|---------------------------|-----------------|-----------------|-----------------|-----------------|-----------------|-----------------|-----------------|
| Accuracy \uparrow | Global | 0.68 \pm 0.16 | 0.75 \pm 0.35 | 0.62 \pm 0.06 | 0.50 \pm 0.00 | 0.54 \pm 0.18 | 0.88 \pm 0.04 |
| | Single-verify | 0.70 \pm 0.21 | 0.75 \pm 0.35 | 0.67 \pm 0.00 | 0.50 \pm 0.00 | 0.67 \pm 0.24 | 0.75 \pm 0.07 |
| | Open-ended | 0.60 \pm 0.06 | - | 0.33 \pm 0.00 | 0.50 \pm 0.00 | 0.50 \pm 0.24 | 1.00 \pm 0.00 |
| | Multiple-choice | 0.68 \pm 0.06 | - | 0.83 \pm 0.24 | 0.50 \pm 0.00 | 0.33 \pm 0.00 | 1.00 \pm 0.00 |
| Macro F1 \uparrow | Global | 0.59 \pm 0.21 | 0.67 \pm 0.47 | 0.55 \pm 0.08 | 0.33 \pm 0.00 | 0.43 \pm 0.23 | 0.87 \pm 0.05 |
| | Single-verify | 0.62 \pm 0.28 | 0.67 \pm 0.47 | 0.62 \pm 0.00 | 0.33 \pm 0.00 | 0.58 \pm 0.35 | 0.74 \pm 0.09 |
| | Open-ended | 0.50 \pm 0.06 | - | 0.18 \pm 0.02 | 0.33 \pm 0.00 | 0.40 \pm 0.22 | 1.00 \pm 0.00 |
| | Multiple-choice | 0.59 \pm 0.08 | - | 0.78 \pm 0.31 | 0.33 \pm 0.00 | 0.17 \pm 0.00 | 1.00 \pm 0.00 |
| Token F1 \uparrow | Global | 0.86 \pm 0.06 | 0.87 \pm 0.19 | 0.90 \pm 0.02 | 0.81 \pm 0.00 | 0.85 \pm 0.05 | 0.88 \pm 0.02 |
| | Single-verify | 0.89 \pm 0.10 | 0.87 \pm 0.19 | 0.93 \pm 0.01 | 0.82 \pm 0.00 | 0.89 \pm 0.08 | 0.97 \pm 0.01 |
| | Open-ended | 0.81 \pm 0.01 | - | 0.79 \pm 0.01 | 0.79 \pm 0.00 | 0.83 \pm 0.04 | 0.83 \pm 0.00 |
| | Multiple-choice | 0.82 \pm 0.01 | - | 0.97 \pm 0.05 | 0.79 \pm 0.00 | 0.79 \pm 0.00 | 0.76 \pm 0.09 |
| Exact Match \uparrow | Global | 0.56 \pm 0.14 | 0.75 \pm 0.35 | 0.62 \pm 0.06 | 0.50 \pm 0.00 | 0.54 \pm 0.18 | 0.47 \pm 0.04 |
| | Single-verify | 0.70 \pm 0.21 | 0.75 \pm 0.35 | 0.67 \pm 0.00 | 0.50 \pm 0.00 | 0.67 \pm 0.24 | 0.75 \pm 0.07 |
| | Open-ended | 0.38 \pm 0.06 | - | 0.33 \pm 0.00 | 0.50 \pm 0.00 | 0.50 \pm 0.24 | 0.20 \pm 0.00 |
| | Multiple-choice | 0.46 \pm 0.06 | - | 0.83 \pm 0.24 | 0.50 \pm 0.00 | 0.33 \pm 0.00 | 0.20 \pm 0.00 |
| BERTScore (F1) \uparrow | Global | 0.89 \pm 0.00 | 0.94 \pm 0.04 | 0.86 \pm 0.03 | 0.88 \pm 0.04 | 0.90 \pm 0.01 | 0.84 \pm 0.01 |
| | Single-verify | 0.93 \pm 0.02 | 0.94 \pm 0.04 | 0.97 \pm 0.02 | 0.93 \pm 0.07 | 1.00 \pm 0.00 | 0.82 \pm 0.01 |
| | Open-ended | 0.78 \pm 0.00 | - | 0.61 \pm 0.01 | 0.83 \pm 0.00 | 0.79 \pm 0.01 | 0.87 \pm 0.01 |
| | Multiple-choice | 0.85 \pm 0.02 | - | 0.89 \pm 0.08 | 0.81 \pm 0.03 | 0.81 \pm 0.03 | 0.87 \pm 0.01 |
| METEOR \uparrow | Global | 0.88 \pm 0.01 | 0.94 \pm 0.04 | 0.86 \pm 0.05 | 0.85 \pm 0.06 | 0.89 \pm 0.01 | 0.82 \pm 0.01 |
| | Single-verify | 0.92 \pm 0.02 | 0.94 \pm 0.04 | 0.93 \pm 0.05 | 0.93 \pm 0.08 | 1.00 \pm 0.00 | 0.81 \pm 0.01 |
| | Open-ended | 0.76 \pm 0.01 | - | 0.67 \pm 0.03 | 0.77 \pm 0.03 | 0.78 \pm 0.01 | 0.83 \pm 0.01 |
| | Multiple-choice | 0.82 \pm 0.02 | - | 0.91 \pm 0.08 | 0.76 \pm 0.05 | 0.79 \pm 0.03 | 0.83 \pm 0.01 |

Table 9: Per-dataset breakdown for in-domain testing (mean \pm std over runs) for the baseline configuration of operaCT on discriminative tasks.

| Metric | Subset | Global | Coswara | CoughVid | ICBHI | KAUH | Respiratory@TR |
|---------------------------|-----------------|-----------------|-----------------|-----------------|-----------------|-----------------|-----------------|
| Accuracy \uparrow | Global | 0.61 \pm 0.02 | 0.59 \pm 0.12 | 0.65 \pm 0.14 | 0.56 \pm 0.09 | 0.47 \pm 0.04 | 0.79 \pm 0.02 |
| | Single-verify | 0.60 \pm 0.03 | 0.59 \pm 0.12 | 0.72 \pm 0.16 | 0.62 \pm 0.18 | 0.53 \pm 0.20 | 0.58 \pm 0.04 |
| | Open-ended | 0.60 \pm 0.06 | - | 0.33 \pm 0.00 | 0.50 \pm 0.00 | 0.50 \pm 0.24 | 1.00 \pm 0.00 |
| | Multiple-choice | 0.68 \pm 0.06 | - | 0.83 \pm 0.24 | 0.50 \pm 0.00 | 0.33 \pm 0.00 | 1.00 \pm 0.00 |
| Macro F1 \uparrow | Global | 0.54 \pm 0.06 | 0.50 \pm 0.24 | 0.58 \pm 0.18 | 0.43 \pm 0.14 | 0.40 \pm 0.03 | 0.77 \pm 0.01 |
| | Single-verify | 0.54 \pm 0.10 | 0.50 \pm 0.24 | 0.69 \pm 0.20 | 0.53 \pm 0.28 | 0.51 \pm 0.17 | 0.54 \pm 0.02 |
| | Open-ended | 0.49 \pm 0.05 | - | 0.17 \pm 0.00 | 0.33 \pm 0.00 | 0.40 \pm 0.22 | 1.00 \pm 0.00 |
| | Multiple-choice | 0.59 \pm 0.08 | - | 0.78 \pm 0.31 | 0.33 \pm 0.00 | 0.17 \pm 0.00 | 1.00 \pm 0.00 |
| Token F1 \uparrow | Global | 0.84 \pm 0.02 | 0.78 \pm 0.07 | 0.91 \pm 0.04 | 0.83 \pm 0.03 | 0.82 \pm 0.02 | 0.89 \pm 0.00 |
| | Single-verify | 0.84 \pm 0.03 | 0.78 \pm 0.07 | 0.93 \pm 0.05 | 0.87 \pm 0.06 | 0.83 \pm 0.06 | 0.96 \pm 0.00 |
| | Open-ended | 0.81 \pm 0.01 | - | 0.79 \pm 0.00 | 0.79 \pm 0.00 | 0.83 \pm 0.04 | 0.83 \pm 0.00 |
| | Multiple-choice | 0.84 \pm 0.01 | - | 0.97 \pm 0.05 | 0.79 \pm 0.00 | 0.79 \pm 0.00 | 0.83 \pm 0.00 |
| Exact Match \uparrow | Global | 0.50 \pm 0.02 | 0.59 \pm 0.12 | 0.65 \pm 0.14 | 0.56 \pm 0.09 | 0.47 \pm 0.04 | 0.39 \pm 0.02 |
| | Single-verify | 0.60 \pm 0.03 | 0.59 \pm 0.12 | 0.72 \pm 0.16 | 0.62 \pm 0.18 | 0.53 \pm 0.20 | 0.58 \pm 0.04 |
| | Open-ended | 0.38 \pm 0.06 | - | 0.33 \pm 0.00 | 0.50 \pm 0.00 | 0.50 \pm 0.24 | 0.20 \pm 0.00 |
| | Multiple-choice | 0.46 \pm 0.06 | - | 0.83 \pm 0.24 | 0.50 \pm 0.00 | 0.33 \pm 0.00 | 0.20 \pm 0.00 |
| BERTScore (F1) \uparrow | Global | 0.87 \pm 0.01 | 0.82 \pm 0.07 | 0.90 \pm 0.03 | 0.87 \pm 0.03 | 0.86 \pm 0.02 | 0.89 \pm 0.02 |
| | Single-verify | 0.90 \pm 0.02 | 0.82 \pm 0.07 | 0.96 \pm 0.03 | 0.90 \pm 0.06 | 0.89 \pm 0.04 | 0.93 \pm 0.01 |
| | Open-ended | 0.82 \pm 0.01 | - | 0.72 \pm 0.00 | 0.83 \pm 0.00 | 0.88 \pm 0.01 | 0.85 \pm 0.03 |
| | Multiple-choice | 0.86 \pm 0.02 | - | 0.96 \pm 0.06 | 0.83 \pm 0.00 | 0.79 \pm 0.00 | 0.85 \pm 0.03 |
| METEOR \uparrow | Global | 0.85 \pm 0.01 | 0.81 \pm 0.06 | 0.89 \pm 0.05 | 0.84 \pm 0.03 | 0.83 \pm 0.02 | 0.88 \pm 0.01 |
| | Single-verify | 0.88 \pm 0.02 | 0.81 \pm 0.06 | 0.91 \pm 0.07 | 0.89 \pm 0.05 | 0.86 \pm 0.06 | 0.94 \pm 0.00 |
| | Open-ended | 0.80 \pm 0.01 | - | 0.77 \pm 0.00 | 0.79 \pm 0.02 | 0.83 \pm 0.05 | 0.81 \pm 0.01 |
| | Multiple-choice | 0.83 \pm 0.02 | - | 0.96 \pm 0.06 | 0.77 \pm 0.00 | 0.77 \pm 0.00 | 0.81 \pm 0.01 |

Table 10: Per-dataset breakdown for in-domain testing (mean \pm std over runs) for RAMoEA-QA on discriminative tasks.

| Metric | Subset | Global | Coswara | CoughVid | ICBHI | KAUH | Respiratory@TR |
|---------------------------|-----------------|-----------------|-----------------|-----------------|-----------------|-----------------|-----------------|
| Accuracy \uparrow | Global | 0.72 \pm 0.02 | 0.86 \pm 0.09 | 0.54 \pm 0.14 | 0.58 \pm 0.15 | 0.68 \pm 0.02 | 0.79 \pm 0.02 |
| | Single-verify | 0.81 \pm 0.00 | 0.86 \pm 0.09 | 0.78 \pm 0.16 | 0.72 \pm 0.22 | 1.00 \pm 0.00 | 0.57 \pm 0.04 |
| | Open-ended | 0.46 \pm 0.02 | - | 0.00 \pm 0.00 | 0.44 \pm 0.09 | 0.33 \pm 0.00 | 1.00 \pm 0.00 |
| | Multiple-choice | 0.62 \pm 0.10 | - | 0.61 \pm 0.24 | 0.44 \pm 0.09 | 0.39 \pm 0.08 | 1.00 \pm 0.00 |
| Macro F1 \uparrow | Global | 0.67 \pm 0.03 | 0.86 \pm 0.09 | 0.51 \pm 0.18 | 0.47 \pm 0.18 | 0.60 \pm 0.02 | 0.75 \pm 0.01 |
| | Single-verify | 0.79 \pm 0.01 | 0.86 \pm 0.09 | 0.76 \pm 0.19 | 0.67 \pm 0.29 | 1.00 \pm 0.00 | 0.51 \pm 0.03 |
| | Open-ended | 0.38 \pm 0.02 | - | 0.00 \pm 0.00 | 0.26 \pm 0.11 | 0.17 \pm 0.00 | 1.00 \pm 0.00 |
| | Multiple-choice | 0.53 \pm 0.12 | - | 0.51 \pm 0.34 | 0.30 \pm 0.04 | 0.23 \pm 0.09 | 1.00 \pm 0.00 |
| Token F1 \uparrow | Global | 0.88 \pm 0.00 | 0.93 \pm 0.05 | 0.88 \pm 0.04 | 0.84 \pm 0.06 | 0.90 \pm 0.00 | 0.83 \pm 0.01 |
| | Single-verify | 0.92 \pm 0.01 | 0.93 \pm 0.05 | 0.95 \pm 0.04 | 0.90 \pm 0.08 | 1.00 \pm 0.00 | 0.83 \pm 0.01 |
| | Open-ended | 0.78 \pm 0.00 | - | 0.71 \pm 0.02 | 0.77 \pm 0.02 | 0.79 \pm 0.00 | 0.84 \pm 0.01 |
| | Multiple-choice | 0.83 \pm 0.02 | - | 0.93 \pm 0.06 | 0.76 \pm 0.04 | 0.80 \pm 0.02 | 0.84 \pm 0.01 |
| Exact Match \uparrow | Global | 0.58 \pm 0.02 | 0.86 \pm 0.09 | 0.54 \pm 0.14 | 0.58 \pm 0.15 | 0.68 \pm 0.02 | 0.34 \pm 0.02 |
| | Single-verify | 0.79 \pm 0.00 | 0.86 \pm 0.09 | 0.78 \pm 0.16 | 0.72 \pm 0.22 | 1.00 \pm 0.00 | 0.47 \pm 0.04 |
| | Open-ended | 0.24 \pm 0.02 | - | 0.00 \pm 0.00 | 0.44 \pm 0.09 | 0.33 \pm 0.00 | 0.20 \pm 0.00 |
| | Multiple-choice | 0.40 \pm 0.10 | - | 0.61 \pm 0.24 | 0.44 \pm 0.09 | 0.39 \pm 0.08 | 0.20 \pm 0.00 |
| BERTScore (F1) \uparrow | Global | 0.89 \pm 0.00 | 0.94 \pm 0.04 | 0.86 \pm 0.03 | 0.88 \pm 0.04 | 0.90 \pm 0.01 | 0.84 \pm 0.01 |
| | Single-verify | 0.93 \pm 0.02 | 0.94 \pm 0.04 | 0.97 \pm 0.02 | 0.93 \pm 0.07 | 1.00 \pm 0.00 | 0.82 \pm 0.01 |
| | Open-ended | 0.78 \pm 0.00 | - | 0.61 \pm 0.01 | 0.83 \pm 0.00 | 0.79 \pm 0.01 | 0.87 \pm 0.01 |
| | Multiple-choice | 0.85 \pm 0.02 | - | 0.89 \pm 0.08 | 0.81 \pm 0.03 | 0.81 \pm 0.03 | 0.87 \pm 0.01 |
| METEOR \uparrow | Global | 0.88 \pm 0.01 | 0.94 \pm 0.04 | 0.86 \pm 0.05 | 0.85 \pm 0.06 | 0.89 \pm 0.01 | 0.82 \pm 0.01 |
| | Single-verify | 0.92 \pm 0.02 | 0.94 \pm 0.04 | 0.93 \pm 0.05 | 0.93 \pm 0.08 | 1.00 \pm 0.00 | 0.81 \pm 0.01 |
| | Open-ended | 0.76 \pm 0.01 | - | 0.67 \pm 0.03 | 0.77 \pm 0.03 | 0.78 \pm 0.01 | 0.83 \pm 0.01 |
| | Multiple-choice | 0.82 \pm 0.02 | - | 0.91 \pm 0.08 | 0.76 \pm 0.05 | 0.79 \pm 0.03 | 0.83 \pm 0.01 |

Table 11: Per-dataset breakdown for in-domain testing (mean \pm std over runs) for the baseline using operaCT on regressive tasks.

| Question-type | Metric | MM Lung | | NoseMic |
|---------------|-------------------|-----------------|-----------------|------------------|
| | | FEV1 | FVC | Respiratory rate |
| Open-ended | MSE \downarrow | 1.11 \pm 0.30 | 3.42 \pm 0.28 | 27.79 \pm 2.34 |
| | RMSE \downarrow | 1.05 \pm 0.14 | 1.85 \pm 0.08 | 5.27 \pm 0.22 |

Table 12: Per-dataset breakdown for in-domain testing (mean \pm std over runs) for the baseline using operaGT on regressive tasks.

| Question-type | Metric | MM Lung | | NoseMic |
|---------------|-------------------|-----------------|-----------------|------------------|
| | | FEV1 | FVC | Respiratory rate |
| Open-ended | MSE \downarrow | 1.13 \pm 0.28 | 2.73 \pm 0.69 | 33.23 \pm 2.01 |
| | RMSE \downarrow | 1.06 \pm 0.13 | 1.65 \pm 0.21 | 5.76 \pm 0.17 |

Table 13: Per-dataset breakdown for in-domain testing (mean \pm std over runs) for RAMoEA-QA on regressive tasks.

| Question-type | Metric | MM Lung | | NoseMic |
|---------------|-------------------|-----------------|-----------------|------------------|
| | | FEV1 | FVC | Respiratory rate |
| Open-ended | MSE \downarrow | 0.96 \pm 0.13 | 2.42 \pm 1.00 | 26.11 \pm 8.09 |
| | RMSE \downarrow | 0.98 \pm 0.07 | 1.54 \pm 0.33 | 5.08 \pm 0.80 |